Science of the Total Environment 772 (2021) 145540

Contents lists available at ScienceDirect

Science of the Total Environment

journal homepage: www.elsevier.com/locate/scitotenv

Revegetation induced change in soil erodibility as influenced by slope situation on the Loess Plateau

Mingming Guo [a,b], Zhuoxin Chen [c], Wenlong Wang [b,c,*], Tianchao Wang [c], Wenxin Wang [c], Zhiqiang Cui [b]

[a] Key Laboratory of Mollisols Agroecology, Northeast Institute of Geography and Agroecology, Chinese Academy of Sciences, Harbin, Heilongjiang 150081, PR China
[b] State Key Laboratory of Soil Erosion and Dryland Farming on the Loess Plateau, Institute of Water and Soil Conservation, Chinese Academy of Sciences and Ministry of Water Resources, Yangling, Shaanxi 712100, PR China
[c] State Key Laboratory of Soil Erosion and Dryland Farming on the Loess Plateau, Institute of Water and Soil Conservation, Northwest A&F University, Yangling, Shaanxi 712100, PR China

HIGHLIGHTS

- Response of soil erodibility to slope situation was explored.
- Soil and root can contribute 69.8%–79.7% of variances in soil erodibility.
- Slope situation affects soil erodibility by altering soil-root feedback relations.
- Three plant models are suggested to reduce soil erodibility along slope situation.

GRAPHICAL ABSTRACT

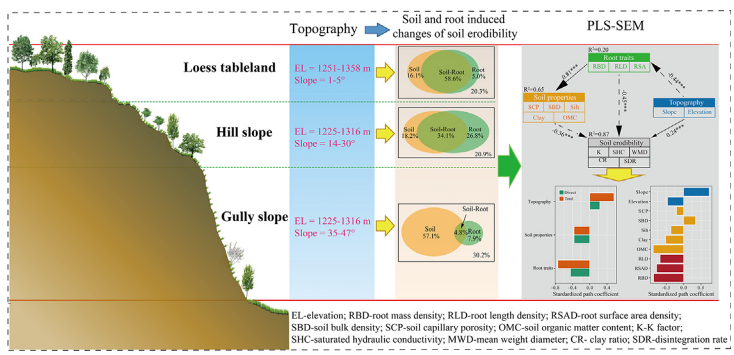

ARTICLE INFO

Article history:
Received 3 December 2020
Received in revised form 26 January 2021
Accepted 27 January 2021
Available online 3 February 2021

Editor: Manuel Esteban Lucas-Borja

Keywords:
Soil erodibility
Landscape position
Land use
Root traits
Soil erosion

ABSTRACT

Soil erodibility is an indispensable parameter for predicting soil erosion and evaluating the benefits of soil and water conservation. Slope situation can alter revegetation and its effects on soil properties and root traits, and thus may affect soil erodibility. However, whether slope situation will change the effect of revegetation on soil erodibility through improving soil properties and root traits has rarely been evaluated. Therefore, this study was conducted to detect the response of soil erodibility to slope situations (loess-tableland, hill-slope and gully-slope) in a typical watershed of the Loess Plateau. Five soil erodibility parameters (saturated soil hydraulic conductivity, *SHC*; mean weight diameter of aggregates, *MWD*; clay ratio, *CR*; soil disintegration rate, *SDR*; soil erodibility factor, *K*) and a comprehensive soil erodibility index (*CSEI*) are selected to clarify the study targets. The results revealed that soil properties, root traits, soil erodibility parameters and *CSEI* were affected by slope situation significantly. Soil and root can explain 79.7%, 79.1% and 69.8% of total variance in soil erodibility of loess-tableland, hill-slope and gully-slope, respectively. Slope situation influenced soil erodibility by changing the effects of revegetation on soil properties and root traits. Evidently, the slope situation greatly changed the relations between *CSEI* and soil and root parameters, whereafter a model considering slope situation (slope steepness), sand, organic matter content and root surface area density was reliable to estimate soil erodibility (*CSEI*). Our study suggested that the *Armeniaca sibirica*, the combination of *Bothriochloa ischcemum* and *Robinia pseudoacacia* and the combination of *Armeniaca sibirica* and *Lespedeza bicolor* can be used as the optimal selection for mitigating soil erodibility of loess-tableland, hill-slope and gully-slope, respectively. This study is of great significance in optimizing the spatial layout of soil and water conservation measures for different slope situations of the Loess Plateau.

* Corresponding author at: State Key Laboratory of Soil Erosion and Dryland Farming on the Loess Plateau, Institute of Water and Soil Conservation, Chinese Academy of Sciences and Ministry of Water Resources, Yangling, Shaanxi 712100, PR China.
E-mail address: nwafu_wwl@163.com (W. Wang).

https://doi.org/10.1016/j.scitotenv.2021.145540
0048-9697/

1. Introduction

Soil erosion seriously threatens ecological environment, agricultural production and sustainable development (Nearing et al., 2000; Zhu et al., 2018). Accurate prediction of soil erosion is extremely important for the deployment of soil and water conservation measures. Soil erodibility is defined as the sensitivity of soil material to erosion (Bryan et al., 1989), and it is an indispensable parameter for estimating soil erosion amount, revealing soil erosion mechanisms and evaluating the benefits of soil and water conservation (Saygin et al., 2018). Consequently, it is critically important to investigate the variations of soil erodibility under different erosive environments.

Soil erodibility was firstly introduced in the Universal Soil Loss Equation (USLE) and expressed as the *K* factor (Zhang et al., 2008). Currently, several popular models (e.g., Geometric Mean Diameter model and Erosion/Productivity Impact Calculator model) are commonly appointed to estimate *K* factor. In addition, some soil properties from different aspects are also widely used to characterize soil erodibility. Saturated soil hydraulic conductivity (*SHC*) reflects soil permeability and is closely related to the sloped runoff characteristics, so it is expected to affect soil erosion (Parsakhoo et al., 2014). Moreover, previous studies have confirmed that *SCH* is an available parameter to characterize soil erodibility (e.g., Cerdà, 1998; Yu et al., 2006). The mean weight diameter of water-stable aggregate (*MWD*) is also a frequently-used parameter to characterize soil structural stability and soil erodibility (Le Bissonnais, 1996). Clay ratio (*CR*) is defined as the ratio of sand and silt content to clay content, and it is popularly used for soil erodibility evaluation (Bouyoucos, 1935; Bryan, 1968; Kusre et al., 2018). Soil disintegration rate (*SDR*) refers to the mass or volume of soil particles separated from original soil in a still water environment per unit time, and it is also frequently used to describe soil erosion resistance (Li et al., 2017; Guo et al., 2018, 2020a, 2020b).

Many studies have revealed that the changes in abovementioned five soil erodibility parameters are significantly affected by basic soil properties and root traits (Chen and Zhou, 2013; Gao et al., 2017; Ostovari et al., 2018). The effects of soil properties and root traits on soil erodibility are mainly reflected in two aspects. Firstly, during the growth of vegetation, roots gradually penetrate into the soil to contribute additional shear strength, thereby weakening soil erodibility (Wang and Zhang, 2017). In addition, many root exudates will adhere to the surface of the soil particles, and the adhesion between root surface and soil particles can be enhanced through the Van der Waals forces (Wang et al., 2018b). Secondly, the vegetation litter and various root exudates in topsoil layer could be converted into soil organic matter, which can improve soil microorganisms' activities and promote the formation of soil aggregates, thus reducing soil erodibility (Forster, 1990; Six et al., 2004; Walia and Dick, 2018). In summary, these advantageous effects of vegetation characteristics on soil properties have been verified to significantly affect soil erodibility (Shit and Maiti, 2012; Li et al., 2017; Wang et al., 2018a).

Previous studies have showed that different revegetation options fundamentally drive the change of land use types and alter soil and root properties, thereby affecting soil erodibility (e.g., Guo et al., 2018; Eghdami et al., 2019; Fayiah et al., 2019). Numerous studies have also clarified the influence of land use change on soil erodibility and confirmed that revegetation is a practical and crucial way to reduce soil erodibility and control soil and water loss (e.g., Boix-Fayos et al., 2001; An et al., 2013). However, which land use and/or plant communities is the most effective in weakening soil erodibility is still controversial. Several studies showed that grassland communities had a greater benefit of reducing soil erodibility (e.g., Li et al., 2015b; Zhang et al., 2019). However, Chen and Zhou (2013) found that the soil erodibility of *Robinia pseudoacacia* (woodland) is less than other land use types. This may be due to differences in erosion environments (e.g., slope situation, climate, vegetation type, soil texture) among different study regions. Therefore, the optimal land use and its corresponding plant communities for reducing soil erodibility need to be clarified in future studies.

Furthermore, it is worth noting that the geomorphology varies greatly in some high-intensity soil erosion regions. Evidently, slope situation is the most important factor controlling soil moisture, and soil moisture greatly changes with terrain heterogeneity (Hawley et al., 1983; Melliger and Niemann, 2010). Gao et al. (2011) concluded that the steep and undulating gully-slopes can provide a harsher water use environment for vegetation growth than hill-slopes. Therefore, the slope situation is expected to influence vegetation growth conditions and its natural succession processes (Cerdà, 1998; Kou et al., 2016), thereby affecting soil properties and erodibility (Ziadat et al., 2010; Zhang et al., 2019). Nevertheless, current research mainly focused on the impacts of land use and its associated plant communities on soil erodibility on single slope situation (gully head, hilly slope or gully slope) (Guo et al., 2018, 2020b; Wang et al., 2018a, 2019a). The lack of systematic evaluation on the influence of land use change induced by revegetation on soil erodibility of different slope situations is not conducive to accurately predict soil erosion and reasonably plan soil and water conservation measures. Therefore, it is critical to clarify how slope situation affects the change in soil erodibility induced by revegetation.

Given the abovementioned scientific gaps, we hypothesized that the plants can alter soil properties during revegetation and further affect soil erodibility, and the effect is controlled by slope situation. Therefore, we selected three typical slope situations (loess-tableland, hill-slope and gully-slope) involving four land uses (farmland, grassland, shrubland and woodland) in a typical watershed of the Loess Plateau with three specific purposes: 1) to illuminate the effects of slope situation on the change in soil erodibility induced by revegetation reflected by *SHC*, *MWD*, *CR*, *SDR*, *K* factor and a comprehensive soil erodibility index (*CSEI*); 2) to clarify the difference in the responses of soil erodibility to soil properties and root traits among three slope situations; and 3) to give a suggestion on the optimal revegetation models for reducing soil erodibility of different slope situations.

2. Materials and methods

2.1. Study area

Our study was carried out in the Nanxiaohegou watershed (35°41′–35°44′N, 107°30′–107°37′E), Qingyang city, China (Fig. 1a). The watershed located in the typical loess-tableland and gully region of the Loess Plateau and covered an area of 36.3 km^2 with an altitude range of 1050 to 1423 m (Fig. 1b). The climate of study area belongs to a temperate continental semi-arid climate with the mean annual temperature of 10 °C. The average annual precipitation of the study area in the past 60 years (1954–2014) is 547 mm, 76.9% of which occurs from May to September (Xia et al., 2017). The main soil type is classified as loessial soil in Chinese Soil Taxonomy which is equivalent to Haplic Cambisols in World Reference Base for Soil Resources (IUSS, 2015). Gully headcut migration is the main reason for serious soil erosion. To contain gully development and protect loess-tableland, the "Three Protection Belts" project was conducted to reduce soil and water loss of gully head, hill-slope and gully channel since 1970s (Zhao, 1994). The "Grain for Green" project was implemented to transform steep sloped-cropland into forest and grass lands since 1999 (Fu et al., 2011). Since then, the land use type has been continuously adjusted, especially the vegetation distribution has undergone tremendous changes (Jiao et al., 2008). At present, the annual soil erosion modulus has been controlled at a lower level (2439 t km^{-2} a^{-1}), and the plants are primarily artificially planted arbors and herbaceous vegetation and shrubs (Guo et al., 2018).

2.2. Identification of loess-tableland, hill-slope and gully-slope

In this study watershed, the geomorphological feature of the three selected slope situations (loess-tableland, hill-slope and gully-slope) is

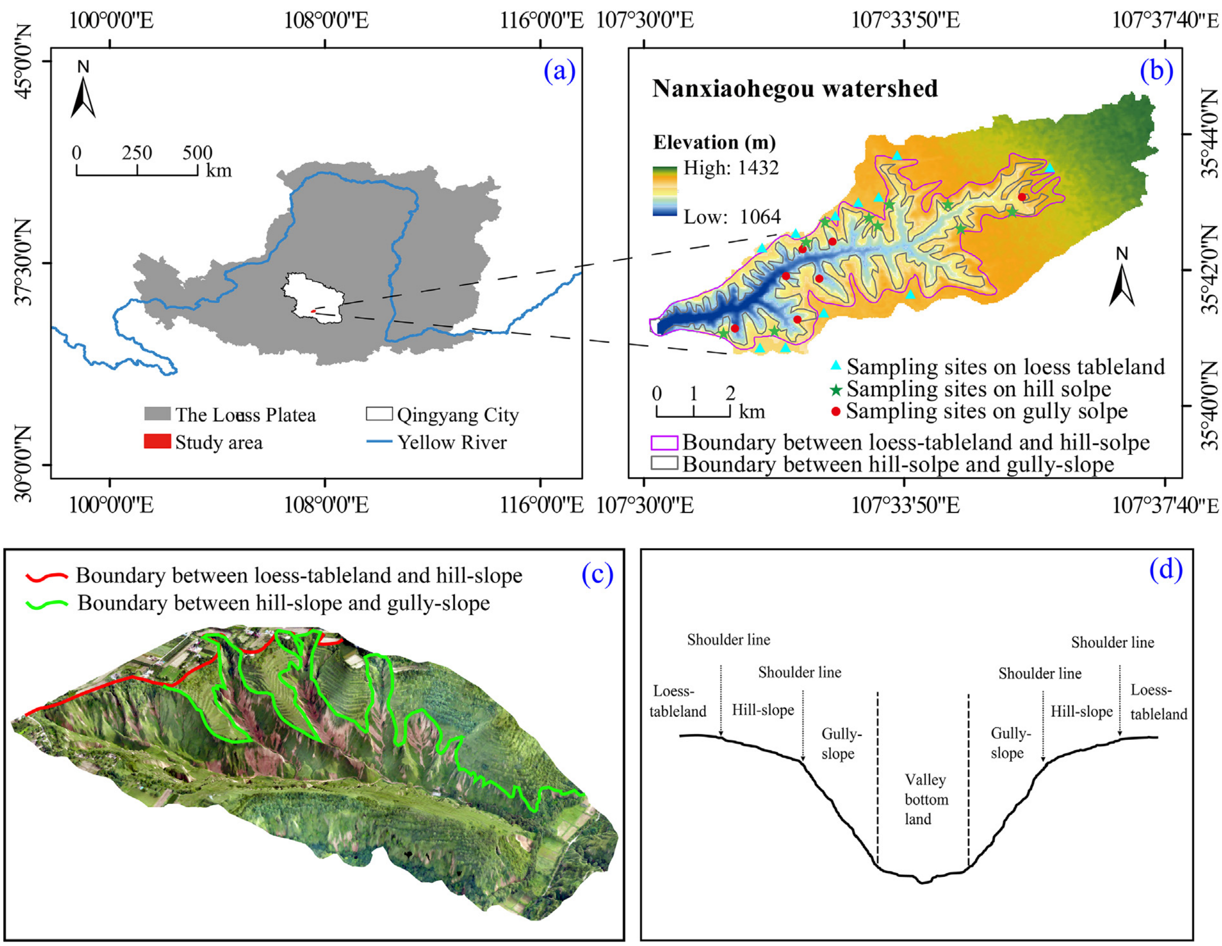

Fig. 1. Location of study area in the Loess Plateau (a), and the distribution of the 28 sampling sites in the study area (b), geomorphological feature in the loess-tableland and gully region of the Loess Plateau (c), and the typical profile illustrating the gully shoulder-line's location (d).

significantly different, and the three slope situations are obviously separated by two clear boundaries (Fig. 1c, d). The area of loess-tableland region accounts for 57% of the study watershed area, and its terrain is flat and the slope is generally less than 5°. The hill-slope area accounts for 16% of the watershed area, and the slope gradient ranges from 5° to 35°. The slope gradient of gully-slope is relatively larger, mostly greater than 35°. Therefore, the 5° and 35° are treated as the critical slope gradient to extract the two shoulder lines for identifying the loess-tableland, hill-slope and gully-slope. Firstly, the DEM (30 m × 30 m) of study watershed was imported into ArcMap software (version 10.2), and the slope raster data (Triangulated Irregular Networks Data) was obtained through the 3D Analysis Tool in the Arc Toolbox. Then, the slope gradient was divided into three categories (<5°, 5–35°, >35°) (Zhu et al., 2003; Song et al., 2013), and the two extracted boundary lines were illustrated in Fig. 1b.

2.3. Selection of sampling sites

From July to September 2018, we investigated in detail the land uses and plant communities of three slope situations (loess-tableland, hill-slope and gully-slope) in the Nanxiaohegou watershed. As a result, 11, 10 and 7 sampling sites were selected on the loess-tableland, hill-slope and gully-slope, respectively (Fig. 1d). In general, the vegetation restoration on loess-tableland is close to the shoulder line between loess-tableland and hill-slope for containing gully head migration. Therefore, the sampling sites on loess-tableland were selected at least 0.5 m away from the shoulder line for sampling safety (Guo et al., 2020b). Consequently, four land uses (11 plant communities) were selected on loess-tableland, including one farmland, five grasslands, two shrublands and three woodlands. Four land uses (10 plant communities) were also selected on the hill-slope, including one farmland, five grasslands, one shrubland and three woodlands. Three land uses (7 plant communities) were selected on gully slope, including three grasslands, one shrubland and three woodlands. It was almost impossible to find slope farmland on gully slope due to the steep slope and implementation of ecological restoration project. Therefore, no farmland sampling site was selected on the gully-slope. It should be noted that these selected sampling sites are the most typical vegetation communities along slope situation. The Table S1 shows the basic information of plant species and topography of 28 sampling sites.

2.4. Sampling and measurement of basic soil and root properties

Three repeated quadrats were established in each sampling site to collect soil and root samplings according to the "S"-shaped sampling method. Firstly, 252 topsoil samples (28 site × 3 quadrats/site × 3 samples/quadrat) were collected from the 0–10 cm soil layer by cutting rings (100 cm^3 in volume), and then these samples were oven-dried to determine soil bulk density (*SBD*) at 105 °C for 24 h. Similarly, another 252 soil samples were collected using steel cutting rings (100 cm^3) to measure soil capillary porosity (*SCP*) (Wang et al., 2013, 2014). In each quadrat, three undisturbed soil samples were collected using a steel cubic box (15 cm in length) and mixed and air-dried in lab, and then the roots, gravel, litter and debris were picked out. As a result, 84 mixed soil samples (28 sampling site × 3 samples/site) were obtained to measure clay content (*Cl*), silt content (*Si*), sand content (*Sa*) and soil organic matter content (*OMC*). The detailed measured methods for *Cl*, *Si*, *Sa* and *OMC* could be referred in many previous studies (e.g., Wang et al., 2013, 2014; Zhu et al., 2010; Guo et al., 2018). In each quadrat, three root samples were taken using a self-made 10 × 10 × 10 cm (length × width × depth) steel box, and a total of 252 root samples (28 sites × 3 quadrats/site × 3 soil samples/quadrat) were acquired. These soil-root samples were firstly placed in water to increase soil dispersion. Then, we washed them with low pressure water and picked all the live roots with tweezers (Guo et al., 2018). The washed live roots were scanned by the Epson V700 Scanner (Seiko Epson Corporation, Nagano Prefecture, Japan) and then the scanned images were analyzed in Win RHIZO image analysis software (version 2007 pro) to indirectly acquire root length density (*RLD*) and root surface area density (*RSAD*). Then, the roots were oven-dried at 65 °C for 48 h and weighed to calculate the root mass density (*RMD*). The measured basic soil and root property parameters were showed in Table S1.

2.5. Determination of soil erodibility parameters

Our study selected five soil erodibility parameters including saturated hydraulic conductivity (*SHC*), soil disintegration rate (*SDR*), mean weight diameter of water-stable aggregate (*MWD*), clay ratio (*CR*) and *K* factor (*K*). The sampling of *SHC*, *SDR*, and *WSA* were also conducted in an 'S'-shaped pattern method. *SDR* is defined as the mass or volume of soil particles separated from original soil dissipated in a static water environment per unit time (Li et al., 2015a, 2017; Guo et al., 2018, 2020b). In this study, 252 soil samples were collected using iron cube boxes (5 cm in side-length) and then were placed in a disintegrating box to measure *SDR* (Guo et al., 2018). Similarly, another 252 soil samples were sampled with cutting ring (200 cm^3) to measure *SHC* by the constant water head height being 5 cm (Hu et al., 2012; Guo et al., 2020a). The sampled 84 mixed soil samples were also used to measure soil water-stable aggregate distribution by an aggregate analyzer with five apertures (0.25, 0.50, 1.0, 2.50 and 5.0 mm) (An et al., 2013). The aggregate fragments left on five sieves were oven-dried and weighted, and then the mean weight diameter (*MWD*) can be calculated by Eq. (1).

$$MWD = \sum_1^n \left(\overline{R_i} w_i\right) / \sum_1^n w_i \tag{1}$$

where $\overline{R_i}$ and w_i are the mean diameter of the *i*-class aggregate and the weight of *i*-class, respectively.

Clay ratio (*CR*) is defined as the ratio of sand and silt content to clay content and is also used to evaluate soil erodibility (Bouyoucos, 1935). *CR* was calculated as follows:

$$CR = (Sa + Si)/Cl \tag{2}$$

where *Sa*, *Si* and *Cl* represent the soil sand content (2–0.05 mm, %), silt content (0.05–0.002 mm, %) and clay content (<0.002 mm, %), respectively.

The *K* factor in USLE was also employed to evaluate soil erodibility, and it was calculated by the EPIC method which was proposed by Williams and Arnold (1997), as shown in Eq. (3).

$$K_{epic} = \left\{0.2 + 0.3 \exp\left[-\frac{0.0256Sa(1-Si)}{100}\right]\right\} \cdot \left(\frac{Si}{Cl + Si}\right)^{0.3} \cdot \left[1.0 - \frac{0.25C}{C + exp(3.72 - 2.95C)}\right] \cdot \left[1.0 - \frac{0.7SN_1}{SN_1 + exp(-5.51 + 22.95SN_1)}\right] \tag{3}$$

where *C* is the organic carbon content (%), $C = 0.583 \times OMC$; $SN_1 = 1 - Sa / 100$; K_{epic} is the *K* factor, and its unit is the US unit standard, which can be converted to the international unit (t ha h MJ^{-1} mm^{-1} ha^{-1}) by multiplying by 0.1317.

Zhang et al. (2008, 2016) suggested that the revised K_{epic} by Eq. (4) can be used to calculate the *K* factor on the Loess Plateau.

$$K = 0.5158 \cdot K_{epic} - 0.01383 \tag{4}$$

To comprehensively evaluate soil erodibility, a comprehensive soil erodibility index (*CSEI*) that reflected comprehensively the above-mentioned five erodibility parameters was introduced and calculated by Eq. (5).

$$CSEI = \sum_i^n K_i \cdot S_i \tag{5}$$

where K_i and S_i are the weight and score of the *i*th soil erodibility parameter, respectively (Wang et al., 2018a).

The *CSEI* was calculated by principal component analysis (PCA) according to the following three steps: (1) selection of parameters: *SHC*, *MWD*, *SDR*, *CR* and *K* are selected as soil erodibility parameters for *CSEI* index calculation; (2) In the principal component analysis, the common factor variance reflects the contribution of a certain parameter to the overall variance. The larger the common factor variance, the higher the contribution. In this study, for each slope situation, the weight of the soil erodibility parameter (K_i value) was calculated as the ratio of the common factor variance of each soil erodibility parameter to the total common factor variance (Table 1); and (3) The value of each soil erodibility parameter is converted into the membership value (0–1), and the maximum value (b) and the minimum value (a) are determined. The membership value (S_i) of each parameter is calculated according to the equations shown in Fig. 2. To a certain extent, the *CSEI* is positively correlated with *SDR*, *CR*, *K*, and thus the membership value of the three parameters is calculated by the *S* function (Fig. 2a). The *CSEI* is negatively correlated with *SHC* and *MWD*, and the membership value of *SHC* and *MWD* is calculated by the inverse *S* function (Fig. 2b).

2.6. Statistical analysis

The one-way analysis of variance (ANOVA) followed by HSD Tukey test was employed to determine the difference in soil properties (*Cl*, *Si*, *Sa*, *SBD*, *SCP*, *OMC*), root traits (*RMD*, *RLD*, *RSAD*), soil erodibility parameters (*K*, *SHC*, *MWD*, *CR*, *SDR*) and a comprehensive soil erodibility index (*CSEI*) among different slope situations, land uses and plant communities. The independence of observations, approximate normal distribution and homogeneity of variances of these parameters were examined and verified before the ANOVA. The correlations between soil erodibility parameters and influencing factors were determined by Pearson correlation method. The contributions of soil, root and their combination to total variance in soil erodibility were determined by Redundancy analysis (RDA), and a Monte Carlo test with 999 permutations was employed to test the significance of the RDA (Peres-Neto et al., 2006). Correlations among CSEI, soil properties and root traits were determined by the Pearson's method, and the simple regression analysis was employed to identify the relationships between CSEI and soil properties and root traits.

According to the previous studies (Henseler et al., 2014; Sarstedt et al., 2016; Hao et al., 2020), the partial least squares structural equation model (PLS-SEM) was used to further identify possible pathways whereby factors control soil erodibility and also to assess the direct

Table 1
Weight of different soil erodibility parameters for calculating *CSEI*.

Slope situation	Item	*K*	*SHC*	*MWD*	*CR*	*SDR*
Loess-tableland	Common factor variance	0.730	0.423	0.806	0.753	0.807
	Weight	0.214	0.124	0.236	0.221	0.236
Hill-slope	Common factor variance	0.842	0.49	0.816	0.457	0.809
	Weight	0.247	0.144	0.239	0.134	0.237
Gully-slope	Common factor variance	0.642	0.811	0.865	0.979	0.865
	Weight	0.154	0.195	0.208	0.235	0.208

Note: *K*, *SHC*, *MWD*, *CR* and *SDR* refer to soil erodibility factor, saturated soil hydraulic conductivity, mean weight diameter, clay ratio and soil disintegration rate, respectively.

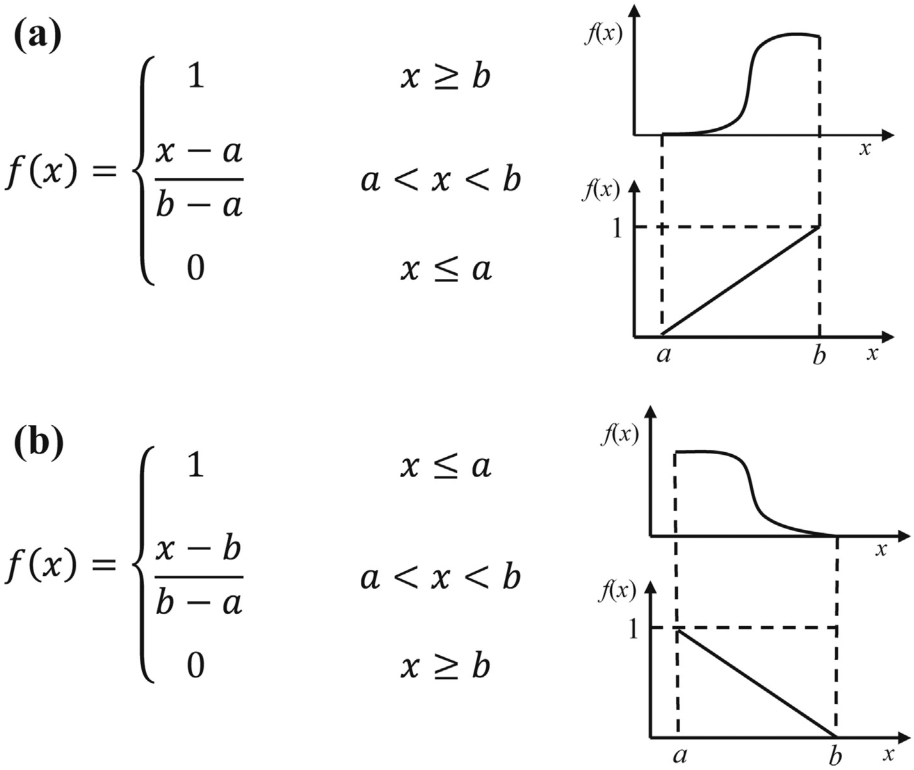

Fig. 2. The relationship between membership function ($f(x)$) and soil erodibility parameters (x) can be described by "S" curve (a) and reverse "S" curve (b). Note: x is the soil erodibility parameter value, and a and b are the lower and upper bounds of soil erodibility parameters.

and indirect effects of topography (elevation, *EL*; slope steepness, *SS*), soil properties, root traits on soil erodibility parameters. The PLS-SEM evaluation is based on the overall model goodness-of-fit index. The models were constructed using the "plspm" package. Significant difference was determined at levels of $P < 0.05$, $P < 0.01$, and $P < 0.001$. All statistical analyses were conducted with the SPSS software (version 16.0), and all figures except for Fig. 1 were produced using R software (version 3.6.3) and Origin software (version 2020a).

3. Results

3.1. Soil properties and root traits along slope situation

Slope situation significantly influenced the majority of soil and root properties (Fig. 3). Loess-tableland had greater clay content (*Cl*) and silt content (*Si*) than hill-slope and gully-slope (Fig. 3a, b), while its sand content (*Sa*) significantly lower than hill-slope and gully-slope (Fig. 3c). Soil bulk density (*SBD*) of gully-slope was significantly 4.1% and 5.8% greater than those of loess-tableland and hill-slope, respectively (Fig. 3d). However, no significant difference in soil capillary porosity (*SCP*) was found among three slope situations (Fig. 3e). Loess-tableland had the maximum organic matter content (*OMC*), which was significantly higher than those of hill-slope and gully-slope (Fig. 3f). The root mass density (*RMD*), root length density (*RLD*) and root surface area density (*RSAD*) on loess-tableland were significantly larger than those on hill-slope and gully-slope (Fig. 3g, h, i), while no significant differences in *RLD* and *RSAD* were found between hill-slope and gully-slope.

3.2. Change in five soil erodibility parameters along slope situation

Fig. 4 illustrates the changes in five soil erodibility parameters along slope situation. The *K* of loess-tableland and hill-slope significantly decreased by 30.3% and 11.8%, respectively, compared with gully-slope (Fig. 4a). The loess-tableland had the largest saturated soil hydraulic conductivity (*SHC*) (0.25 mm min^{-1}), followed by gully-slope and hill-slope (Fig. 4b). The mean weight diameter (*MWD*) of gully-slope was minimum (0.85 mm), and it was significantly less than that of loess-tableland but showed a non-significant difference with that of hill-slope (Fig. 4c). The minimum clay ratio (*CR*) found in loess-tableland was significantly less than those of other two slope situations (Fig. 4d). The soil disintegration rate (*SDR*) of gully-slope was 1.40 times and 1.01 times significantly greater than those of loess-tableland and hill-slope, whereas the *SDR* values between loess-tableland and hill-slope are slightly different (Fig. 4e). Overall, the five soil erodibility parameters increased from up to low slope situations.

For a given slope situation, the land use also greatly influenced soil erodibility (Fig. 5). On the loess-tableland, the lowest *K* value found in shrubland was significantly lower than that of farmland (Fig. 5a), but the *SHC* showed a non-significant change among four land use types (Fig. 5b). Compared with farmland, the *MWD*s of the three revegetated land uses increased significantly by 48.7%–69.3%, but there was no significant difference among the three revegetated land uses (Fig. 5c). Changes in *CR* and *SDR* with land use were the exact opposite of *MWD* (Fig. 5d, e). Similarly, on the hill-slope, the *K* values of three restored land uses significantly decreased by 11.1%–17.8% compared with farmland (Fig. 5f). Woodland had the largest *SHC* (0.25 mm min^{-1}), followed by grassland, shrubland and farmland (Fig. 5g). After revegetation, the *MWD* significantly increased by 0.38–1.29 times, of which the woodland showed the maximum increase, followed by shrubland and grassland (Fig. 5h). We found the revegetation affected the *CR* weakly (Fig. 5i), whereas the conversion of farmland to vegetated land uses can significantly decrease *SDR* by 61.9%–82.5%, especially in the woodland (Fig. 5j). On the gully-slope, however, the most of soil erodibility parameters showed a weak change among three vegetated land uses. The woodland had a significantly lower *K* than grassland and shrubland (Fig. 5k), however, the difference in *SHC* among grassland, shrubland and woodland did not reach a significant level (Fig. 5l). The *MWDs* of shrubland and woodland were significantly greater than that of grassland by 65.8% and 37.4%, respectively (Fig. 5m). Similar to loess-

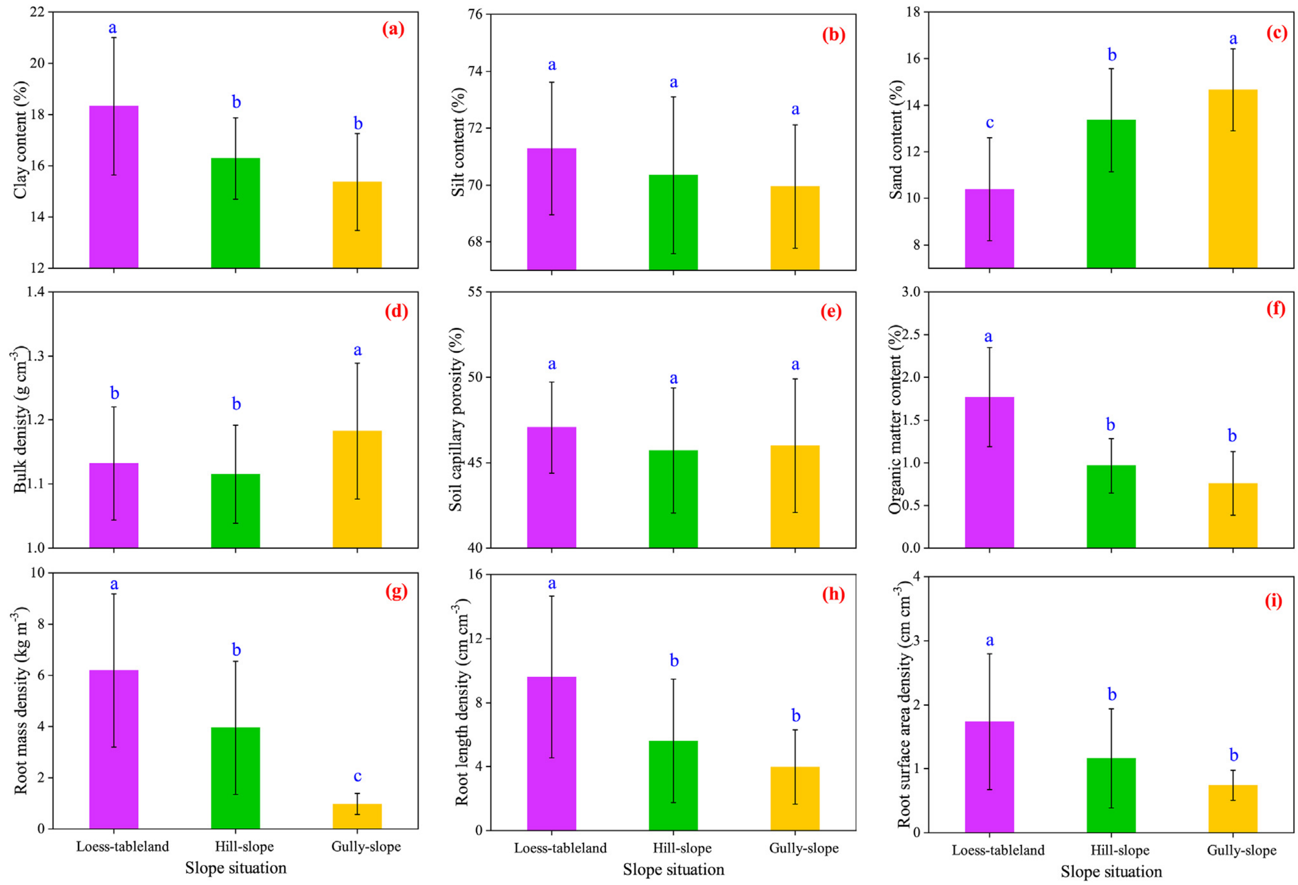

Fig. 3. Variations in basic soil and root properties of different slope situations.

tableland and hill-slope, the *CR* was not affected by land use (Fig. 5n), but the shrubland had a significantly lower *SDR* (0.92 g min^{-1}) than grassland and woodland (Fig. 5n).

3.3. Contributions of soil and root to the variation of soil erodibility

The redundancy analysis (RDA) followed by Monte Carlo permutation test revealed that the variations in five soil erodibility parameters were influenced significantly by soil and root properties on the three slope situations ($P < 0.01$, Fig. 6). On the loess-tableland, the 79.7% of total variance can be explained by soil and root properties, with soil properties, root traits and the combination of soil and root explaining 16.1%, 5.0%, and 58.6% of the total variance, respectively. For the hill-slope, the soil and root can contribute 79.1% of the total variance of soil erodibility (Fig. 6b), of which soil, root and their combination accounted 18.2%, 26.8%, and 34.1% of the total variance, respectively. However, on the gully-slope, only the 69.8% of total variance in soil erodibility could be explained by soil and root properties, of which soil properties driven the most of variability (57.1%) and root and the combination of soil and root only contributed 7.9% and 4.7% of total variance, respectively (Fig. 6c).

Our conceptual model significantly explained 87% of the change in soil erodibility, with a goodness of fit of 0.58. Root traits were the factors that directly influenced soil erodibility with a standardized path coefficient (SPC) of −0.45 (Fig. 7a), followed by basic soil properties (SPC = −0.36) and topography factor (SPC = 0.24). The total effect of root traits on soil erodibility was highest with the SPC of −0.74 that resulted from the significant effects of root systems on soil properties. The total effect of topography on soil erodibility was positive (SPC = 0.56) that was mainly derived from direct effect (SPC = 0.24) and indirect effect (SPC = 0.33) via plant root system (Fig. 7b). The cross-loading effects also can show the differentiation among different factors in the PLS-SEM model (Fig. 7c). Only the slope steepness and soil bulk density displayed the positive effects on soil erodibility with SPCs of 0.74 and 0.34, respectively. However, with respect to the negative effects, we found the OMC exhibited the highest negative effect on soil erodibility (SPC = −0.87), followed by RBD (SPC = −0.86), RSAD (SPC = −0.78), RLD (SPC = −0.67), Cl (SPC = −0.51), elevation (SPC = −0.46), Si (SPC = −0.36), and SCP (SPC = −0.20).

3.4. Change in comprehensive soil erodibility index (CSEI)

The results from Sections 3.2 and 3.3 showed that the five soil erodibility parameters and its response to influencing factors exhibited a significant different change along slope situation. Therefore, the *CSEI* comprehensively considering five soil erodibility parameters was employed to evaluate the effects of slope situation, land use and plant community on soil erodibility (Fig. 8).

The gully-slope had the maximum *CSEI* (0.72), and it was significantly larger than that of loess-tableland but exhibited a non-significant difference with that of hill-slope (Fig. 8a). Overall, the soil erodibility reflected by *CSEI* increased from the up to down slope situations. For a given slope situation, the land use type also greatly affected *CSEI*. On the loess-tableland, compared with farmland, only the *CSEI* of the woodland significantly decreased by 8.0% (Fig. 8b). On the hill-slope, the *CSEI* of farmland was the highest, and it was significantly higher than that of woodland (Fig. 8c). In addition, we found that no significant difference in *CSEI* was obtained among farmland, grassland and shrubland ($P > 0.05$), although *CSEI*s of grassland and shrubland were less than that of farmland. Similarly, for the gully-slope, the woodland had the significantly lower *CSEI* (0.67) than grassland and shrubland (Fig. 8d).

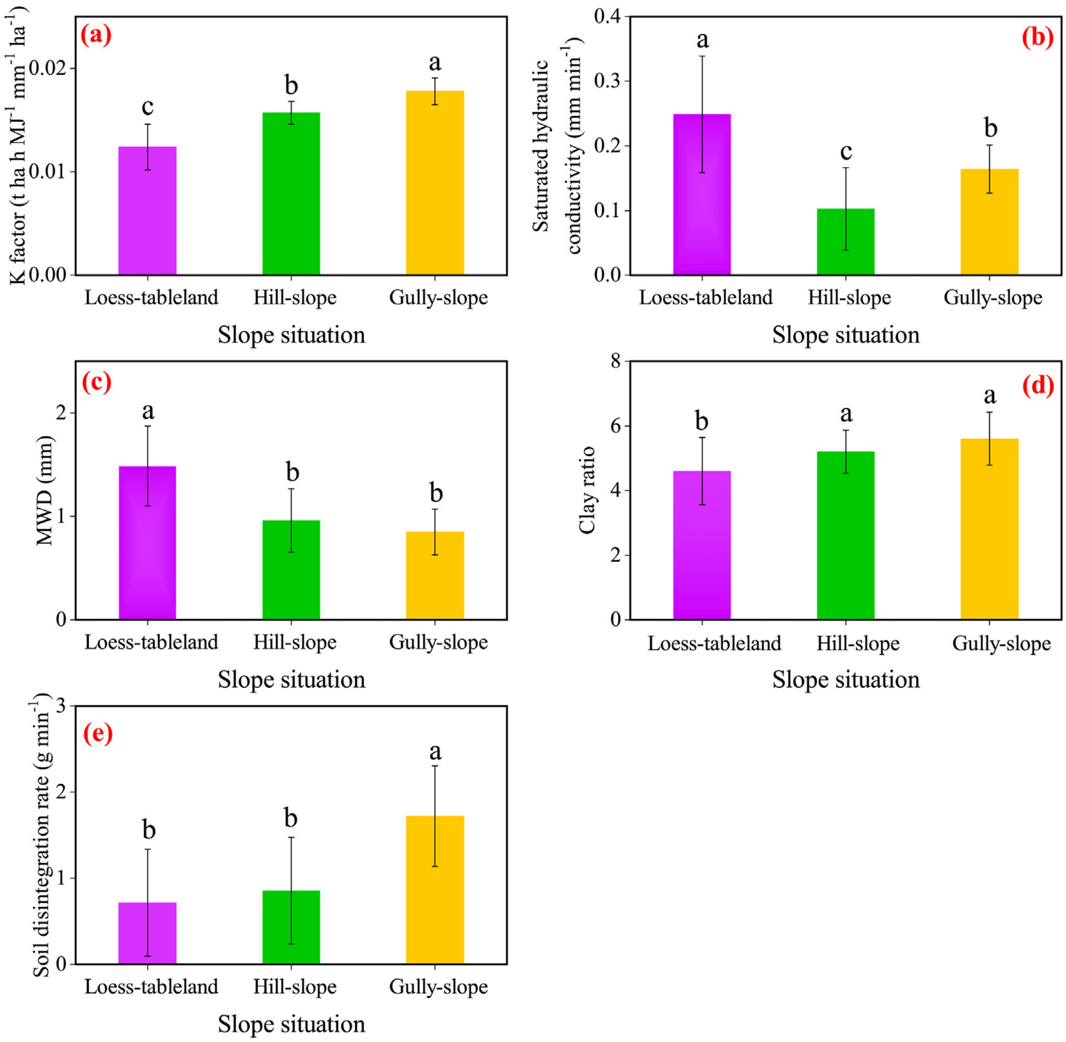

Fig. 4. Variations in five soil erodibility parameters along slope situation.

The difference in *CSEI* among different plant communities was compared to determine the optimal revegetation model on each slope situation. On the loess-tableland, the LGBY grassland site (*Bothriochloa ischcemum*) and LWSX woodland site (*Armeniaca sibirica*) had the relatively lower *CSEI*s that were significantly less than those of the other sites except for *Herba Artimisiae Sieversianae* (LGBH) (Fig. 9a); thus, the two plant communities can be determined as the optimal revegetation models to reduce soil erodibility of loess-tableland. For the hill-slope, only a grassland site (*Bothriochloa ischcemum*, HGBY) and the three woodland sites showed the significantly lower *CSEI*s than the other sites, of which the woodland site (HWCH) dominated by *Robinia pseudoacacia* had the minimum *CSEI*; and thus, the combination of forest and grass (*Bothriochloa ischcemum* and *Robinia pseudoacacia*) should be preferred as revegetation species (Fig. 9b). On the gully-slope, the three woodlands showed relatively lower *CSEI*s than the three grasslands and a shrubland (Fig. 9c). The GWCH dominated by *Robinia pseudoacacia* had the lowest *CSEI* and could be as the first choice for reducing soil erodibility of gully-slope.

3.5. Response relationships between CSEI and soil and root

The *CSEI* of each slope situation was significantly and negatively related to *OMC*, *RBD*, *RLD*, and *RSAD*, but significantly and positively related to *Sa* and slope steepness (*SS*) ($P < 0.05$, Table 2). The *SBD* only significantly affect the *CSEI* of loess-tableland, and the clay and *SCP* only related to *CSEI* of gully-slope ($P < 0.05$), but the Si had no significant effect of *CSEI* of three slope situations ($P > 0.05$). Regression analysis revealed that the *CSEI* linearly increased with the increase of *SS* (Fig. S1a) but linearly decreased with *OMC* increased (Fig. S1c). The positive logarithmical functions can be used to express the changes in *CSEI* of three slope situations with *Sa* (Fig. S1b), whereas the *CSEI* logarithmically or linearly decreased with the increase of three root trait parameters (Fig. S1d–f). In terms of all slopes, we found the *CSEI* was significantly correlated with all soil, root and topography factors (Table 2). A non-linear regression analysis showed the *CSEI* could be well estimated by *SS*, *Si*, *OMC* and *RSAD* (Eq. (6)). This result seemed satisfactory because of the high coefficient of determination ($R^2 = 0.805$), and less scatter was observed around the fitted line (Fig. S2).

$$CSEI = 0.174SS^{0.072} \cdot \ln(Sa + 22.51) \cdot \exp(-0.095OMC - 0.043RSAD), \quad R^2 = 0.804, N = 84, P < 0.001 \tag{6}$$

4. Discussion

4.1. Changes in soil and root along slope situation

Our study quantified the significant effect of slope situation on soil properties and root traits (Fig. 3 and Table S1). The loess-tableland had finer soil texture (higher *Cl* and *Si* and lower *Sa*) than hill-slope and gully-slope (Fig. 3), which confirmed previous erosion-related

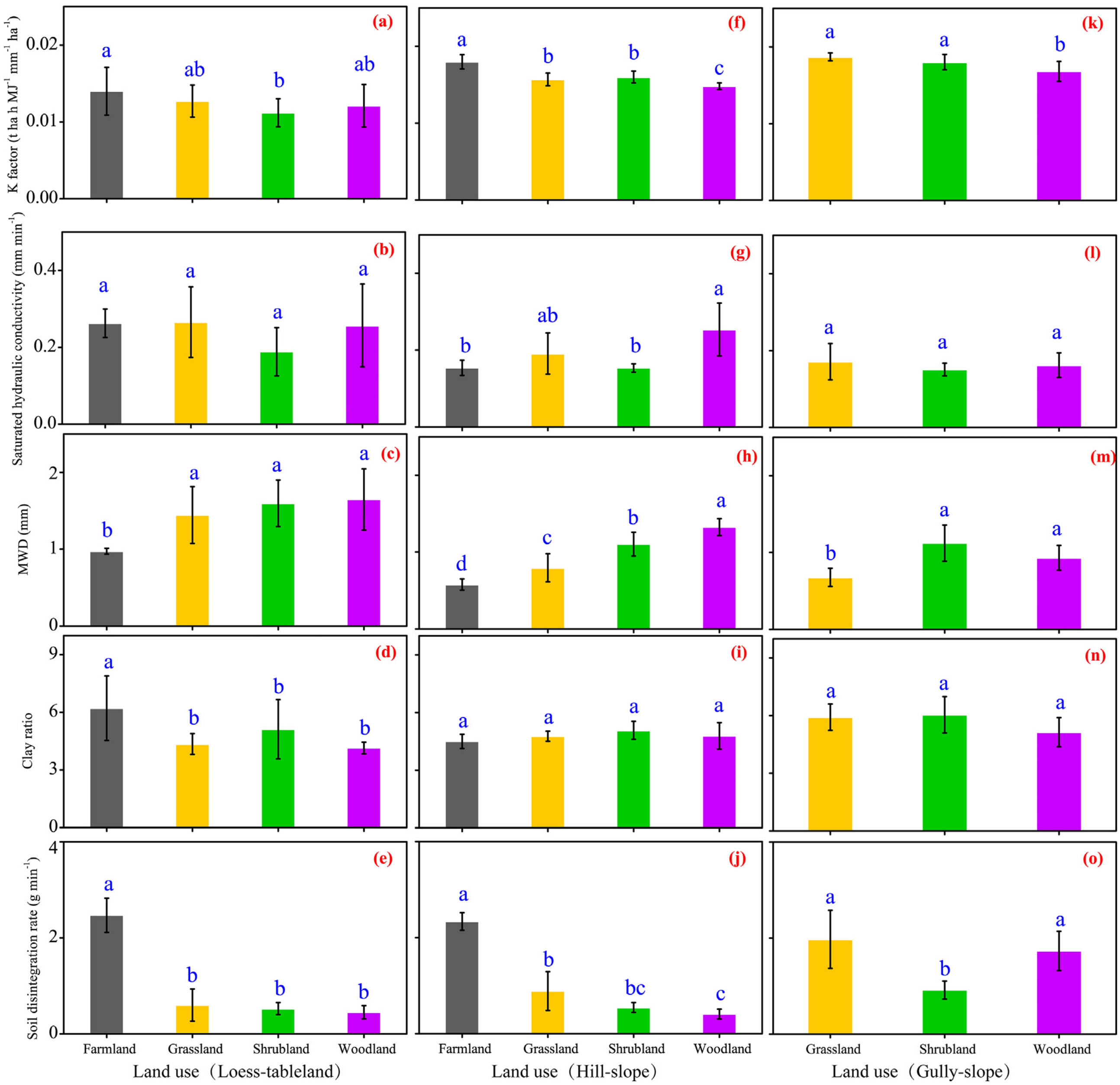

Fig. 5. Change in five soil erodibility parameters with land use along slope situation.

studies showing that gully-slope was subject to more serious soil erosion than loess-tableland and hill-slope and resulted in soil coarsening of gully-slope (Beuselinck et al., 2000; Wang et al., 2019b). The severe erosion on gully-slope also caused the higher soil bulk density and poor soil porosity structure than loess-tableland and hill-slope (Neris et al., 2012). Soil organic matter (*OMC*) is commonly considered as an important parameter influencing soil erosion (Knapen et al., 2007; Guo et al., 2018; Zhang et al., 2019). Our data showed that *OMC* decreased from top to down slope situation, indicating that the lower slope of loess-tableland not only can maintain more rainfall water that was conducive to plant growth causing the litter accumulation on topsoil and the decomposition of plant litter and dead roots (Wang et al., 2018a) but also cause less loss of the soil, litter and humus in topsoil (Sun et al., 2016). Overall, the loess-tableland had the best soil properties, followed by hill-slope and gully-slope, and root density also showed a similar change along slope situation (Fig. 3), which, in fact, was closely related to a complicated plant-soil feedback system induced by revegetation (Miki, 2012; Lucas-Borja et al., 2016; Wu et al., 2016). The better soil properties can provide a better soil environment for plant growth, and in turn, the better growing plants also can produce larger root density and more litter that was conducive to the improvement of soil properties.

4.2. Effect of slope situation on soil erodibility

Our study revealed that slope situation significantly affected five soil erodibility parameters and *CSEI* (Figs. 4, 8a). Overall, soil erodibility increased gradually from up to low slope situations, which is consistent with the result of Wang et al. (2019b) who stated the soil detachment capacity on hillslopes of permanent gullies gradually increased from up to down landscape positions under same erosion condition. However, Geng et al. (2017) found that soil erodibility decreased gradually from up to low landscape positions. This disagreement may be associated with the differences in erosion characteristics, vegetation types, soil and root properties between two study areas. The study of Geng et al. (2017) mainly focused on the sheet, rill, ephemeral gully, and

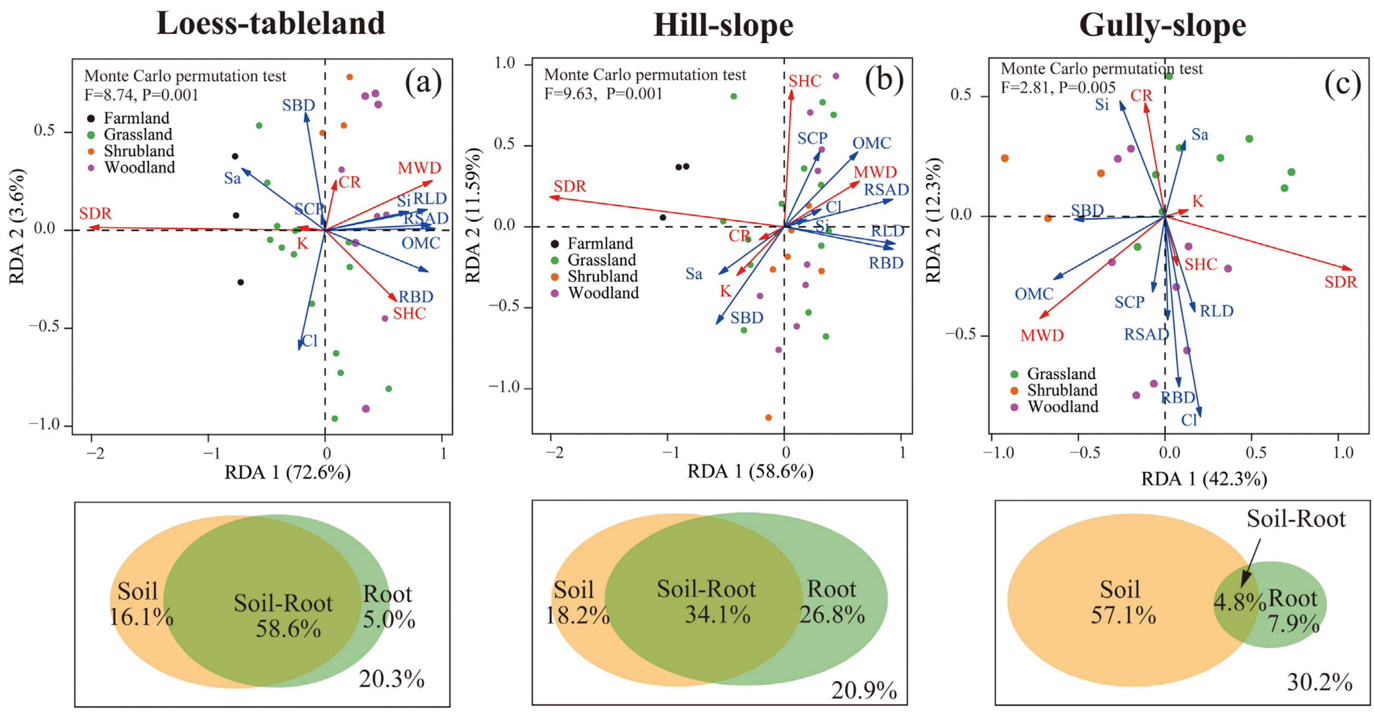

Fig. 6. Results of redundancy analysis (RDA) among soil erodibility parameters and soil and root properties on three slope situations. Note: Cl, Si, Sa, SBD, SCP, OMC, RBD, RLD, RSAD, K, SHC, MWD, CR, SDR and CSEI refer to clay content, silt content, sand content, soil bulk density, soil capillary porosity, organic matter content, root mass density, root length density, soil surface area density, K factor, saturated soil hydraulic conductivity, mean weight diameter of water-stable aggregate, clay ratio, soil disintegration rate and comprehensive soil erodibility index, respectively.

gully erosion in the hilly and gully region of the Loess Plateau, while the erosion characteristics of three slope situations of this study were gully erosion in the loess tableland and gully region the Loess Plateau. In addition, we found the distinct differences in basic soil property, root density and vegetation community among the two studies.

The significant difference in soil erodibility among three slope situations was closely related to difference in topographical feature. In general, soil moisture decreased with the increasing distance along gully-shoulder line and slope gradient (Qiu et al., 2001; Hébrard et al., 2006; Bi et al., 2008). Specifically, for a given rainfall condition, surface runoff easily generated on gully-slope due to low soil permeability (Fig. 4b), and the runoff and soil water drained quickly due to high slope gradient (Fitzjohn et al., 1998; Melliger and Niemann, 2010), which meant that the loess-tableland with lower slope gradient had the relatively higher soil water storage. Therefore, the loess-tableland can provide a relatively better soil moisture environment for plant growth, which was conducive to the improvement of root density and soil properties (Lawless et al., 2008; Duan et al., 2016). From the erosion perspective, the hill-slope and gully-slope had the larger slope gradient and the lower infiltration capacity than loess-tableland, implying that the larger runoff rate was generated easily and quickly on hill-slope and gully-slope and had larger runoff transport capacity under same rainfall condition (Ali et al., 2013). As a result, the hill-slope and gully-slope were subject to more serious soil erosion, and thus, the losses of organic matter, humus and nutrient in topsoil and litter in land surface are more severe than loess-tableland, which would provide a harsher soil environment for plant growth, resulting in higher soil erodibility of hill-slope and gully-slope than that of loess-tableland. Soil moisture is a crucial factor in controlling the process of vegetation restoration (Jian et al., 2015; Hupet and Vanclooster, 2002), and further influenced soil erodibility (Zhang et al., 2019). Therefore, how to strengthen revegetation and reasonably use soil water resource of different slope situations to decrease soil erodibility is a scientific issue worthy of further consideration on the Loess Plateau.

4.3. Contributions of soil and root to change in soil erodibility as affected by slope situation

Soil erodibility is the inherent soil property that is inseparably affected by basic soil characteristics and external environmental factors (Bryan, 2000; Gyssels et al., 2005; Wu et al., 2018). Our data analysis showed that the soil properties and root traits explained significantly the 79.7%, 79.1% and 69.8% of total variances in soil erodibility, and the soil, root, and their combination revealed markedly different explanations among three slope situations (Fig. 6), indicating that the responses of soil erodibility to soil and root was controlled by slope situation significantly. This observation was supported by some previous studies (e.g., Kara and Baykara, 2014; Li et al., 2015b). The PLS-SEM model quantitatively revealed that the slope situation (reflected by *EL* and *SS*) effects on erodibility was obtained mainly by affecting plant growth and root traits (Fig. 7a). Simultaneously, the model also confirmed that the root traits had the greatest effect on soil erodibility by improving soil properties (Fig. 7b). Lots of erosion-related studies unanimously supported the positive and significant effects of vegetation on mitigation of soil erodibility or improvement of soil erosion resistance (De Baets et al., 2006; Burylo et al., 2012; Vannoppen et al., 2015; Guo et al., 2018, 2020a). Besides, in our case, we found that only the *SS* and *SBD* displayed the positive effects on soil erodibility, and other soil and root factors showed the negative effects, which was a little different from the results of Hao et al. (2020) who stated that *Cl*, *Si* and specific root length had the positive effects on erodibility. This controversial result may due to the longer revegetation time, which involved complex ecosystem processes among climate, landscape, plant species, and soil texture (Duyck et al., 2012; Rodriguez-Caballero et al., 2013; Hao et al., 2020).

With regard to the mechanism of erodibility mitigation induced by revegetation, in fact, the change in soil erodibility depended on the soil-root feedback relationship. The root structural systems, as the dynamic interface between soil and vegetation, not only absorbed nutrients

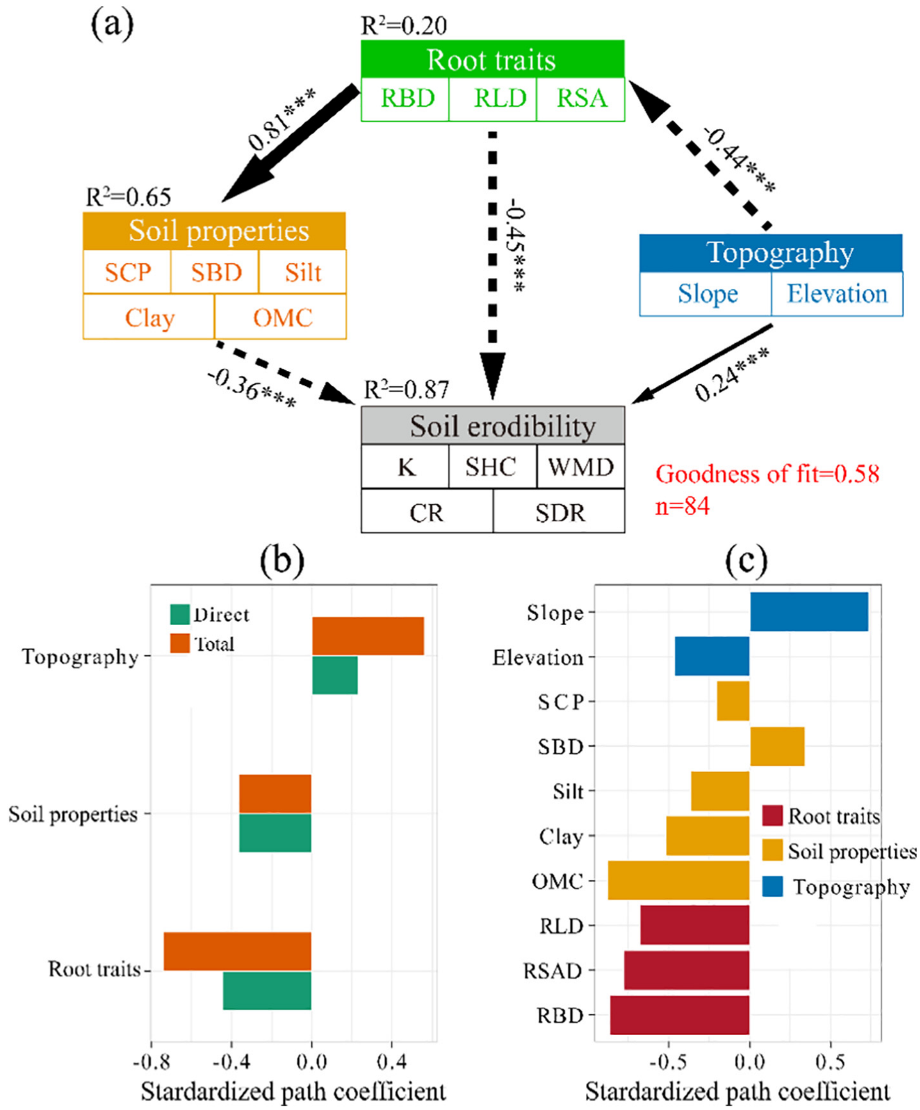

Fig. 7. Diagrammatize method for the effect of the topography (elevation and slope steepness), soil properties (clay, silt, SBD, SCP, OMC), root traits (RBD, RLD, and RSA) on soil erodibility. (a) The PLS-SEM model outputs. (b) The standardized path coefficients for direct and total effects of topography, soil properties, and root traits on soil erodibility. (c) The cross-loading effects of each topography, soil and root parameter in SEM model on soil erodibility. Note: SBD, soil bulk density; SCP, soil capillary porosity; OMC, soil organic matter content; RBD, root mass density; RLD, root length density; RSAD, root surface area density. Number on arrow indicates standardized path coefficient, solid arrow is positive and dashed is negative (significant levels are *<0.05, **<0.01 and ***<0.001). R^2 indicates the variance explained by the model.

from the soil to supply the aboveground growth, but also gradually improved the intrinsic properties of the soil through the existence of the root layer (Zhang et al., 2019; Guo et al., 2020b). The positive root system effect on soil erodibility was mainly due to root bonding effect (Li et al., 2015a). Specifically, the diverse root exudates, mainly carbohydrates, amino acids, organic acids and enzymes, can effectively optimize soil porosity structure, improve soil cohesion and increase soil organic matter, nutrient substances and soil microorganism species, and thus improve soil infiltration capacity and soil structure stability and reduce soil disintegration capacity, *CR* and *K* factor (McDonald et al., 2002; Wang et al., 2013; Li et al., 2017). In turn, the variations of soil properties caused by revegetation also influenced the succession of plant community (Herbrich et al., 2018; Heydari et al., 2020). Our results also proved that the change in soil erodibility strongly depended on the feedback mechanism or interaction between plant and soil (Fig. 6), and the PLS-SEM further indicated that slope situation greatly affected soil erodibility by altering the plant-soil feedback relationship (Fig. 7). Therefore, slope situation is a critical factor influencing soil erodibility (Wang et al., 2019a, b; Geng et al., 2021). Also, the scientific and reasonable spatial planning of vegetation restoration measures should be well-designed and carried out based on the difference in slope situations to further control soil and water loss and improve the quality of ecological environment of the Loess Plateau.

4.4. Response of CSEI to soil properties and root traits

Our study showed the distinct difference in correlations between *CSEI* and soil properties and root traits among three slope situations (Table 2), indicating the slope situation significantly affected the response of soil erodibility to soil and plant root systems (Geng et al., 2017). Moreover, we found that the slopes of the fitted equations between *CSEI* and *SS* and *OMC* all decreased from up to down slope situation (Fig. S1), but the gully-slope had the larger slopes of fitted equations between *CSEI* and *Sa* and the three root trait parameters than those for loess-tableland and hill-slope (Fig. S1). This fully signified that the sensitivity of soil erodibility to *SS* and *OMC* declined along slope situation from top to down, and the response of soil erodibility of gully-slope to the changes in *Sa* and root traits was more sensitive than loess-tableland and hill-slope. When considering all slope situations, we found that *Cl*, *Si*, *Sa*, *SS* and *EL* showed the stronger correlation with

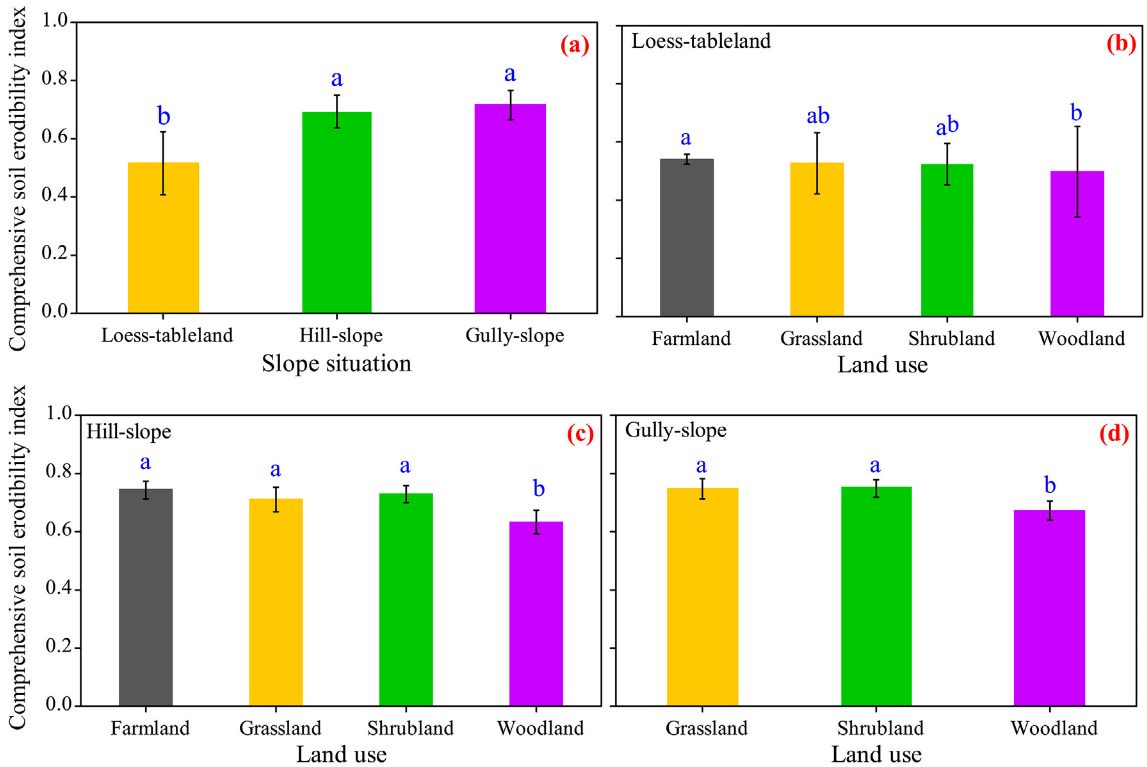

Fig. 8. Variation in comprehensive soil erodibility index with slope situation and land use.

CSEI, fully manifesting the slope situation is a vital factor influencing soil erodibility via altering soil properties and root traits (Martz, 1992; Ziadat et al., 2010; Wang and Zhang, 2021). Furthermore, the soil erodibility reflected by *CSEI* involving all slope situations could be predicted by *SS*, *Si*, *OMC* and *RSAD* (Fig. S2). The *SS* as the slope situation factor is applied to the prediction of soil erodibility. However, Geng et al. (2017) suggested the median soil grain size (D_{50}), soil cohesion, *WSA* and *RMD* are the optimal parameters for predicting soil erodibility. This difference may be due to the great difference in landforms between this study and their study, which altered the effect of revegetation on soil, root and erodibility. In general, it is time-consuming and labor-costing to measure a series of soil erodibility parameters for calculating *CSEI* (Sheridan et al., 2000; Geng et al., 2021). The Eq. (6) in this study can accurately and conveniently estimate *CSEI* using four relatively easily measured soil and root parameters, and thus it can be used as an available approach to estimate soil erodibility of all slopes in this study region.

4.5. Optimal selection of revegetation model for mitigating soil erodibility along slope situation

Our study concluded that revegetation could be confirmed as an effective measure to mitigate soil erodibility (Zhang et al., 2019), and the optimal land use and plant species for reducing soil erodibility were significantly different among three slope situations. Therefore, the selection of land use and its corresponding plant species for reducing soil erodibility should be seriously considered according to the difference in slope situation on the Loess Plateau. The comprehensive soil erodibility (CSEI), fully considering various soil erodibility parameters, was assigned to clear the optimal models of different slope situations. The comparison recommended strongly that the *Armeniaca sibirica*, the combination of *Bothriochloa ischcemum* and *Robinia pseudoacacia*, and the combination of *Armeniaca sibirica* and *Lespedeza bicolor* could be used as the first-choice revegetation models for mitigating soil erodibility of loess-tableland, hill-slope and gully-slope, respectively. This selection was supported by some studies (e.g., Korkanc et al., 2008; Duan et al., 2016; Wang et al., 2019a), and was also different from some previous studies (e.g., Li et al., 2015b; Wei et al., 2007; Zhang et al., 2019). The differentiation was probably mainly caused by different plant communities that was determined by the different erosion environments (e.g., climate, rainfall, topographic conditions, seed bank, soil texture) (Jiao et al., 2008; Liu et al., 2018; Wang et al., 2018b). It's worth noting that the herbaceous vegetation on gully-slope easily caused severe shallow landslide and soil erosion under extreme rainfall conditions (Guo et al., 2020c). Therefore, we should cautiously consider the use of herbaceous vegetation as the main revegetation species on the steep gully-slope. Fortunately, our recommendation (combination of *Armeniaca sibirica* [grass] and *Lespedeza bicolor* [shrub]) satisfied this requirement.

4.6. Limitations and significance of this study

Soil erodibility is an indispensable parameter in the field of soil erosion (Saygin et al., 2018), and the slope situation is an important factor driving vegetation restoration progress and affecting soil erodibility. This study clarified the response of soil erodibility to slope situation and its relationships with soil properties and root traits in a typical watershed of the loess-tableland and gully region. Moreover, an empirical model was developed and well estimated soil erodibility of all slopes. However, there is a potential limitation of single watershed sampling design combined with a relatively small sample size of sites. Thus, further studies should be conducted in more typical watersheds of the study region to make the results of this study more reliable and universally applicable. The empirical equation also needs to be calibrated for estimating soil erodibility of other areas of the Loess Plateau. Although the earlier-noted imperfection represents a limitation of our study, we clearly identified the effect of slope situation on soil erodibility and developed a model for predicting soil erodibility of different slope situations by using some easily measured topography, soil and root parameters. More important, our study recommends the optimal revegetation models for reducing soil erodibility of loess-tableland, hill-slope and gully-slope, which is of great guiding significance for reasonably collocating vegetation measures on different slope situations.

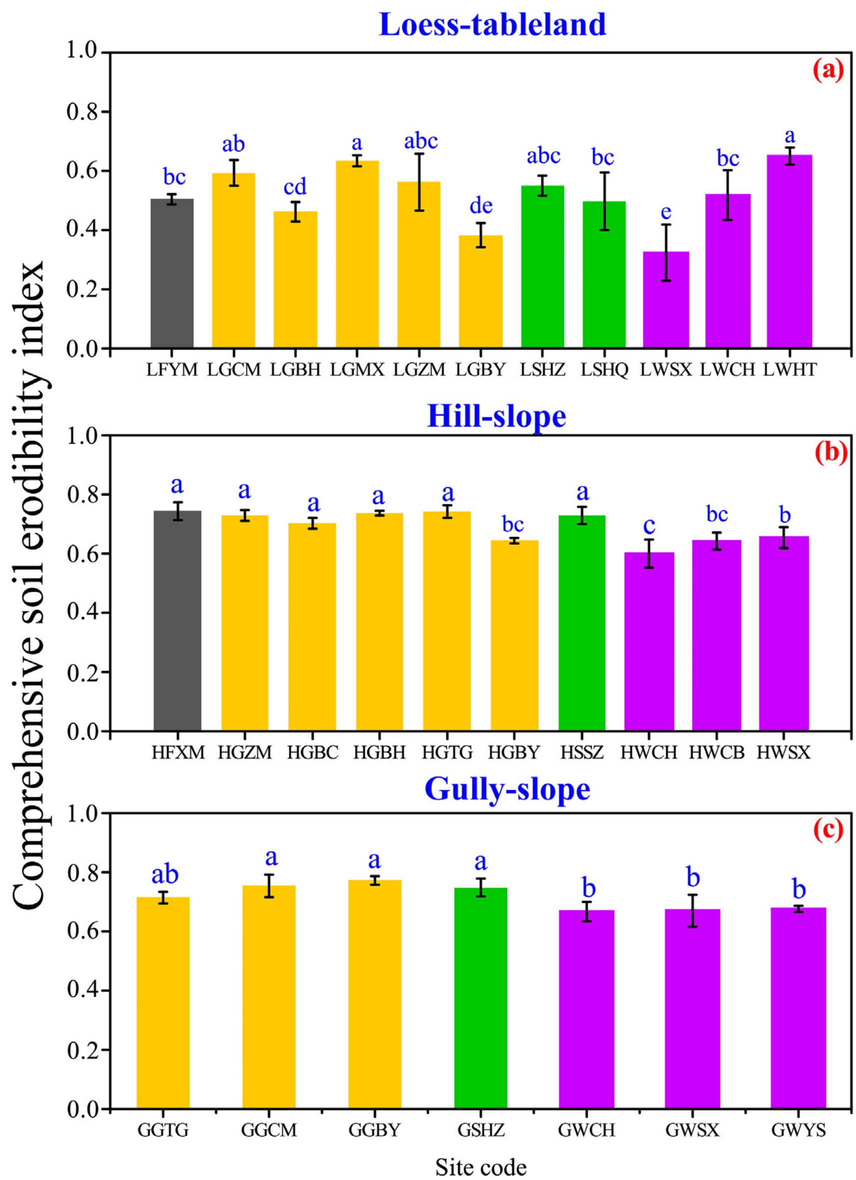

Fig. 9. Difference in comprehensive soil erodibility index among different vegetation communities on different slope situations. Note: LFYM, *Zea may*; LGCM, *Stipa bungeana*; LGBH, *Herba Artimisiae Sieversianae*; LGMX, *Medicago sativa*; LGZM, *Artemisia scoparia*; LGBY, *Bothriochloa ischaemum*; LSHZ, *Lespedeza bicolor*; LSHQ, *Hippophae rhamnoides*; LWSX, *Armeniaca sibirica*; LWCH, *Robinia pseudoacacia*; LWHT, *Juglans regia*; HFXM, *Z. may*; HGZM, *A. scoparia*; HGBC, *Agropyron cristatum*; HGBH, *H. Artimisiae Sieversianae*; HGTG, *Artemisia gmelinii*; HGBY, *B. ischaemum*; HSSZ, *Ziziphus jujuba* var. *spinosa*; HWCH, *R. pseudoacacia*; HWCB, *Platycladus orientalis*; HWSX, *A. sibirica*; GGTG, *A. gmelinii*; GGCM, *S. bungeana*; GGBY, *B. ischaemum*; GSHZ, *L. bicolor*; GWCH, *R. pseudoacacia*; GWSX, *A. sibirica*; GWYS, *Populus tomentosa*.

Table 2
Correlations between comprehensive soil erodibility index and soil properties and root traits in different slope situation.

Slope situation	Soil properties					Root traits				Topography		N
	Cl	Si	Sa	SBD	SCP	OMC	RBD	RLD	RSAD	SS	EL	
Loess-tableland	−0.02	−0.29	0.43**	0.57**	−0.30	−0.75**	−0.42*	−0.35*	−0.68**	0.46**	−0.06	33
Hill-slope	0.30	−0.25	0.58**	0.30	−0.26	−0.55**	−0.63**	−0.65**	−0.55**	0.43*	0.12	30
Gully-slope	−0.46*	−0.002	0.50**	0.30	−0.53*	−0.51*	−0.63**	−0.86**	−0.60**	0.78**	0.08	21
All slopes	−0.38**	−0.38**	0.68**	0.33**	−0.21	−0.85**	−0.65**	−0.57**	−0.68**	0.75**	−0.53**	84

Note: Cl, clay content; Si, silt content; Sa, sand content; SBD, soil bulk density; SCP, soil capillary porosity; OMC, soil organic matter content; RBD, root mass density; RLD, root length density; RSAD, root surface area density; SS, slope steepness; EL, elevation. Significant levels are *<0.05 and **<0.01. N is the sample number.

5. Conclusions

We found that soil properties and root traits changed significantly along the slope situation. Soil erodibility reflected by *K*, *SHC*, *MWD*, *CR*, and *SDR* was also affected by slope situation and land use. The variations of soil erodibility parameters were significantly affected by soil and root, and the soil and root can contribute 79.7%, 79.1% and 69.8% of total variances in soil erodibility of loess-tableland, hill-slope and gully-slope, respectively. The PLS-SEM revealed that the slope situation significantly affected soil erodibility by altering plant (root) growth and its induced soil properties. Furthermore, the *CSEI* also showed significant changes with slope situations, as well as land uses and plant communities, and the slope situation strongly changed the relationships between *CSEI* and soil properties and root traits. An empirical model involving *SS*, *Sa*, *OMC* and *RSAD* was recommended to estimate soil erodibility (*CSEI*). Besides, the *Armeniaca sibirica*, the combination of *Bothriochloa ischcemum* and *Robinia pseudoacacia* and the combination of *Armeniaca sibirica* and *Lespedeza bicolor* strongly recommended as the preferred restoration species for reducing soil erodibility of loess-tableland, hill-slope and gully-slope, respectively. This study is of great guiding significance for the rational planning of revegetation measures on different slope situations of the Loess Plateau.

Supplementary data to this article can be found online at https://doi.org/10.1016/j.scitotenv.2021.145540.

CRediT authorship contribution statement

Mingming Guo: Conceptualization, Validation, Investigation, Writing – original draft, Writing – review & editing, Funding acquisition. **Zhuoxin Chen:** Methodology, Software, Formal analysis, Data curation. **Wenlong Wang:** Conceptualization, Methodology, Writing – review & editing, Visualization, Supervision, Project administration, Funding acquisition. **Tianchao Wang:** Investigation, Resources, Data curation. **Wenxin Wang:** Investigation. **Zhiqiang Cui:** Investigation, Resources.

Declaration of competing interest

The authors declare that they have no known competing financial interests or personal relationships that could have appeared to influence the work reported in this paper.

Acknowledgements

Thanks for the anonymous reviewers' comments. This study was funded by the National Natural Science Foundation of China (42077079, 41571275) and China Postdoctoral Science Foundation (2020M681062).

References

Ali, M., Seeger, M., Sterk, G., Moore, D., 2013. A unit stream power based sediment transport function for overland flow. Catena 101, 197–204. https://doi.org/10.1016/j.catena.2012.09.006.
An, S.S., Darboux, Frédéric, Cheng, M., 2013. Revegetation as an efficient means of increasing soil aggregate stability on the Loess Plateau (China). Geoderma 209–210, 75–85. https://doi.org/10.1016/j.geoderma.2013.05.020.
Beuselinck, L., Steegen, A., Govers, G., Nachtergaele, J., Poesen, J., 2000. Characteristics of sediment deposits formed by intense rainfall events in small catchments in the Belgian loam belt. Geomorphology 32, 69–82. https://doi.org/10.1016/S0169-555X(99)00068-9.
Bi, H., Zhang, J., Zhu, J., Lin, L., Guo, C., Ren, Y., 2008. Spatial dynamics of soil moisture in a complex terrain in the semi-arid Loess Plateau region, China. J. Am. Water Resour. Assoc. 44, 1121–1131. https://doi.org/10.1111/j.1752-1688.2008.00236.x.
Boix-Fayos, C., Calvo-Cases, A., Imeson, A.C., Soriano-Soto, M.D., 2001. Influence of soil properties on the aggregation of some mediterranean soils and the use of aggregate size and stability as land degradation indicators. Catena 44, 47–67. https://doi.org/10.1016/S0341-8162(00)00176-4.
Bouyoucos, G.J., 1935. The clay ratio as a criterion of susceptibility of soils to erosion. J. Am. Soc. Agron. 27, 738–741.
Bryan, R.B., 1968. The development, use and efficiency of indices of soil erodibility. Geoderma 2, 5–26. https://doi.org/10.1016/0016-7061(68)90002-5.
Bryan, R.B., 2000. Soil erodibility and processes of water erosion on hillslope. Geomorphology 32, 385–415. https://doi.org/10.1016/S0169-555X(99)00105-1.
Bryan, R.B., Govers, G., Poesen, J., 1989. The concept of soil erodibility and some problems of assessment and application. Catena 16, 393–412. https://doi.org/10.1016/0341-8162(89)90023-4.
Burylo, M., Rey, F., Mathys, N., Dutoit, T., 2012. Plant root traits affecting the resistance of soils to concentrated flow erosion. Earth Surf. Process. Landf. 37, 1463–1470. https://doi.org/10.1002/esp.3248.
Cerdà, A., 1998. The influence of geomorphological position and vegetation cover on the erosional and hydrological processes on a Mediterranean hillslopes. Hydrol. Process. 12, 661–671. https://doi.org/10.1002/(SICI)1099-1085(19980330)12:4<661::AID-HYP607>3.0.CO;2-7.
Chen, X.Y., Zhou, J., 2013. Volume-based soil particle fractal relation with soil erodibility in a small watershed of purple soil. Environ. Earth Sci. 70, 1735–1746. https://doi.org/10.1007/s12665-013-2261-y.
De Baets, S., Poesen, J., Gyssels, G., Knapen, A., 2006. Effects of grass roots on the erodibility of topsoils during concentrated flow. Geomorphology 76, 54–67. https://doi.org/10.1016/j.geomorph.2005.10.002.
Duan, L., Huang, M., Zhang, L., 2016. Use of a state–space approach to predict soil water storage at the hillslope scale on the Loess Plateau, China. Catena 137, 563–571. https://doi.org/10.1016/j.catena.2015.11.003.
Duyck, P., Dortel, E., Tixier, P., 2012. Niche partitioning based on soil type and climate at the landscape scale in a community of plant-feeding nematodes. Soil Biol. Biochem. 44, 49–55. https://doi.org/10.1016/j.soilbio.2011.09.014.
Eghdami, H., Azhdari, G., Lebailly, P., Azadi, H., 2019. Impact of land use changes on soil and vegetation characteristics in Fereydan, Iran. Agriculture 9, 1–17. https://doi.org/10.3390/agriculture9030058.
Fayiah, M., Dong, S., Li, Y., Xu, Y., Gao, X., Li, S., Shen, H., Xiao, J., Yang, Y., Wessell, K., 2019. The relationships between plant diversity, plant cover, plant biomass and soil fertility vary with grassland type on Qinghai-Tibetan Plateau. Agric. Ecosyst. Environ. 286, 106659. https://doi.org/10.1016/j.agee.2019.106659.
Fitzjohn, C., Ternan, J.L., Williams, A.G., 1998. Soil moisture variability in a semi-arid gully catchment: implications for runoff and erosion control. Catena 32, 55–70. https://doi.org/10.1016/S0341-8162(97)00045-3.
Forster, S.M., 1990. The role of microorganisms in aggregate formation and soil stabilization: types of aggregation. Arid Soil Res. Rehabil. 4, 85–98. https://doi.org/10.1080/15324989009381236.
Fu, B.J., Liu, Y., Lu, Y.H., He, C.S., Zeng, Y., Wu, B.F., 2011. Assessing the soil erosion control service of ecosystems change in the Loess Plateau of China. Ecol. Complex. 8, 284–293. https://doi.org/10.1016/j.ecocom.2011.07.003.
Gao, L.Q., Bowker, M.A., Xu, M.X., Sun, H., Tuo, D.F., Zhao, Y.G., 2017. Biological soil crusts decrease erodibility by modifying inherent soil properties on the Loess Plateau, China. Soil Biol. Biochem. 105, 49–58. https://doi.org/10.1016/j.soilbio.2016.11.009.
Gao, X.D., Wu, P.T., Zhao, X.N., Shi, Y.G., Wang, J.W., Zhang, B.Q., 2011. Soil moisture variability along transects over a well-developed gully in the Loess Plateau, China. Catena 87, 357–367. https://doi.org/10.1016/j.catena.2011.07.004.
Geng, R., Zhang, G.H., Ma, Q.H., Wang, H., 2017. Effects of landscape positions on soil resistance to rill erosion in a small catchment on the Loess Plateau. Biosyst. Eng. 160, 95–108. https://doi.org/10.1016/j.biosystemseng.2017.06.001.
Geng, R., Zhang, G.H., Hong, D.L., Ma, Q.H., Jin, Q., Shi, Y.Z., 2021. Response of soil detachment capacity to landscape positions in hilly and gully regions of the Loess Plateau. Catena 196, 104852. https://doi.org/10.1016/j.catena.2020.104852.
Guo, M.M., Wang, W.L., Kang, H.L., Yang, B., 2018. Changes in soil properties and erodibility of gully heads induced by vegetation restoration on the Loess Plateau, China. J. Arid Land 10, 712–725. https://doi.org/10.1007/s40333-018-0121-z.
Guo, M.M., Wang, W.L., Kang, H.L., Yang, B., Li, J.M., 2020a. Changes in soil properties and resistance to concentrated flow across a 25-year passive restoration chronosequence of grasslands on the Chinese Loess Plateau. Restor. Ecol. 28, 104–114. https://doi.org/10.1111/rec.13057.
Guo, M.M., Wang, W.L., Wang, T.C., Wang, W.X., Kang, H.L., 2020b. Impacts of different vegetation restoration options on gully head soil resistance and soil erosion in loess tablelands. Earth Surf. Process. Landf. 45, 1038–1050. https://doi.org/10.1002/esp.4798.
Guo, W.Z., Chen, Z.X., Wang, W.L., Gao, W.W., Guo, M.M., Kang, H.L., Li, P.F., Wang, W.X., Zhao, M., 2020c. Telling a different story: the promote role of vegetation in the initiation of shallow landslides during rainfall on the Chinese Loess Plateau. Geomorphology 350, 106879. https://doi.org/10.1016/j.geomorph.2019.106879.
Gyssels, G., Poesen, J., Bochet, E., Li, Y., 2005. Impact of plant roots on the resistance of soils to erosion by water: a review. Prog. Phys. Geogr. 29, 189–217. https://doi.org/10.1191/0309133305pp443ra.
Hao, H., Cheng, L., Guo, Z., Wang, L., Shi, Z., 2020. Plant community characteristics and functional traits as drivers of soil erodibility mitigation along a land degradation gradient. Land Degrad. Dev. 31, 1851–1863. https://doi.org/10.1002/ldr.3579.
Hawley, M.E., Jackson, T.J., Mccuen, R.H., 1983. Surface soil moisture variation on small agricultural watersheds. J. Hydrol. 62, 179–200. https://doi.org/10.1016/0022-1694(83)90102-6.
Hébrard, O., Voltz, M., Andrieux, P., Moussa, R., 2006. Spatio-temporal distribution of soil surface moisture in a heterogeneously farmed mediterranean catchment. J. Hydrol. 329, 110–121. https://doi.org/10.1016/j.jhydrol.2006.02.012.
Henseler, J., Dijkstra, T.K., Sarstedt, M., Ringle, C.M., Diamantopoulos, A., Straub, D.W., Calantone, R.J., 2014. Common beliefs and reality about PLS. Organ. Res. Methods 17, 182–209. https://doi.org/10.1177/1094428114526928.
Herbrich, M., Gerke, H.H., Sommer, M., 2018. Root development of winter wheat in erosion-affected soils depending on the position in a hummocky ground moraine soil landscape. J. Plant Nutr. Soil Sci. 181, 147–157. https://doi.org/10.1002/jpln.201600536.

Heydari, M., Zeynali, N., Omidipour, R., Bazgir, M., Kohzadian, M., Prevosto, B., 2020. Linkage between plant species diversity and soil-based functions along a post-agricultural succession is influenced by the vegetative forms. Environ. Monit. Assess. 192, 429. https://doi.org/10.1007/s10661-020-08378-z.

Hu, W., Shao, M.A., Si, B.C., 2012. Seasonal changes in surface bulk density and saturated hydraulic conductivity of natural landscapes. Eur. J. Soil Sci. 63, 820–830. https://doi.org/10.1111/j.1365-2389.2012.01479.x.

Hupet, F., Vanclooster, M., 2002. Intraseasonal dynamics of soil moisture variability within a small agricultural maize cropped field. J. Hydrol. 261, 86–101. https://doi.org/10.1016/S0022-1694(02)00016-1.

IUSS Working Group WRB, 2015. World reference base for soil resources 2014, update 2015 international soil classification system for naming soils and creating legends for soil maps. World Soil Resources Reports. 106. FAO, Rome.

Jian, S.Q., Zhao, C.Y., Fang, S.M., Kai, Y., 2015. Effects of different vegetation restoration on soil water storage and water balance in the Chinese Loess Plateau. Agric. For. Meteorol. 206, 85–96. https://doi.org/10.1016/j.agrformet.2015.03.009.

Jiao, J.Y., Tzanopoulos, J., Xofis, P., Mitchley, J., 2008. Factors affecting distribution of vegetation types on abandoned cropland in the hilly-gullied Loess Plateau region of China. Pedosphere 18, 24–33. https://doi.org/10.1016/S1002-0160(07)60099-X.

Kara, O., Baykara, M., 2014. Changes in soil microbial biomass and aggregate stability under different land uses in the northeastern Turkey. Environ. Monit. Assess. 186, 3801–3808. https://doi.org/10.1007/s10661-014-3658-0.

Knapen, A., Poesen, J., Govers, G., Gyssels, G., Nachtergaele, J., 2007. Resistance of soils to concentrated flow erosion: a review. Earth-Sci. Rev. 80, 75–109. https://doi.org/10.1016/j.earscirev.2006.08.001.

Korkanc, S.Y., Ozyuvaci, N., Hizal, A., 2008. Impacts of land use conversion on soil properties and soil erodibility. J. Environ. Biol. 29, 363–370. https://doi.org/10.2112/05-0545.1.

Kou, M., Jiao, J., Yin, Q., Wang, N., Wang, Z., Li, Y., 2016. Successional trajectory over 10 years of vegetation restoration of abandoned slope croplands in the hill-gully region of the Loess Plateau. Land Degrad. Dev. 27, 919–932. https://doi.org/10.1002/ldr.2356.

Kusre, B.C., Parmita, G., Kishan, N., 2018. Prioritization of soil conservation measures using erodibility indices as criteria in Sikkim (India). J. Earth Syst. Sci. 127, 81. https://doi.org/10.1007/s12040-018-0981-9.

Lawless, C., Semenov, M.A., Jamieson, P.D., 2008. Quantifying the effect of uncertainty in soil moisture characteristics on plant growth using a crop simulation model. Field Crop Res. 106, 138–147. https://doi.org/10.1016/j.fcr.2007.11.004.

Le Bissonnais, Y., 1996. Aggregate stability and assessment of soil crustability and erodibility: I. Theory and methodology. Eur. J. Soil Sci. 47, 425–437. https://doi.org/10.1111/j.1365-2389.1996.tb01843.x.

Li, Q., Liu, G.B., Zhang, Z., Tuo, D.F., Xu, M.X., 2015a. Effect of root architecture on structural stability and erodibility of topsoils during concentrated flow in hilly Loess Plateau. Chin. Geogr. Sci. 25, 757–764. https://doi.org/10.1007/s11769-014-0723-0.

Li, Q., Liu, G.B., Zhang, Z., Tuo, D.F., Bai, R.R., Qiao, F.F., 2017. Relative contribution of root physical enlacing and biochemistrical exudates to soil erosion resistance in the Loess soil. Catena 153, 61–65. https://doi.org/10.1016/j.catena.2017.01.037.

Li, Z.W., Zhang, G.H., Geng, R., Wang, H., 2015b. Rill erodibility as influenced by soil and land use in a small watershed of the Loess Plateau, China. Biosyst. Eng. 129, 248–257. https://doi.org/10.1007/s11769-014-0723-0.

Liu, S.L., Hou, X.Y., Yang, M., Cheng, F.Y., Coxixo, A., Wu, X., Zhang, Y.Q., 2018. Factors driving the relationships between vegetation and soil properties in the Yellow River Delta, China. Catena 165, 279–285. https://doi.org/10.1016/j.catena.2018.02.004.

Lucas-Borja, M.E., Hedo, J., Cerda, A., Candel-Perez, D., Vinegla, B., 2016. Unravelling the importance of forest age stand and forest structure driving microbiological soil properties, enzymatic activities and soil nutrients content in Mediterranean Spanish black pine (*Pinus nigra Ar.* ssp *salzmannii*) forest. Sci. Total Environ. 562, 145–154. https://doi.org/10.1016/j.scitotenv.2016.03.160.

Martz, L.W., 1992. The variation of soil erodibility with slope position in a cultivated Canadian prairie landscape. Earth Surf. Process. Landf. 17, 543–556. https://doi.org/10.1002/esp.3290170602.

McDonald, M.A., Healey, J.R., Stevens, P.A., 2002. The effects of secondary forest clearance and subsequent land-use on erosion losses and soil properties in the Blue Mountains of Jamaica. Agric. Ecosyst. Environ. 92, 1–19. https://doi.org/10.1016/S0167-8809(01)00286-9.

Melliger, J.J., Niemann, J.D., 2010. Effects of gullies on space–time patterns of soil moisture in a semiarid grassland. J. Hydrol. 389, 289–300. https://doi.org/10.1016/j.jhydrol.2010.06.006.

Miki, T., 2012. Microbe-mediated plant–soil feedback and its roles in a changing world. Ecol. Res. 27, 509–520. https://doi.org/10.1007/s11284-012-0937-5.

Nearing, M., Romkens, M., Norton, L., Stott, D., Rhoton, F., Laflen, J., Flanagan, D., Alonso, C., Binger, R., Dabney, S., 2000. Measurements and models of soil loss rates. Science 290, 1300–1301. https://doi.org/10.1126/science.290.5495.1300b.

Neris, J., Jiménez, C., Fuentes, J., Morillas, G., Tejedor, M., 2012. Vegetation and land-use effects on soil properties and water infiltration of Andisols in Tenerife (Canary Islands, Spain). Catena 98, 55–62. https://doi.org/10.1016/j.catena.2012.06.006.

Ostovari, Y., Ghorbani-Dashtaki, S., Bahrami, H.A., Abbasi, M., Dematte, A.M., Arthur, E., Panagos, P., 2018. Towards prediction of soil erodibility, SOM and $Caco_3$ using laboratory Vis-NIR spectra: a case study in a semi-arid region of Iran. Geoderma 314, 102–112. https://doi.org/10.1016/j.geoderma.2017.11.014.

Parsakhoo, A., Lotfalian, M., Ataollah, K., Hosseini, A.S., 2014. Assessment of soil erodibility and aggregate stability for different parts of a forest road. J. For. Res. 25, 193–200. https://doi.org/10.1007/s11676-014-0445-2.

Peres-Neto, P.R., Legendre, P., Dray, S., Borcard, D., 2006. Variation partitioning of species data matrices: estimation and comparison of fractions. Ecology 87, 2614–2625. https://doi.org/10.1890/0012-9658(2006)87[2614:VPOSDM]2.0.CO;2.

Qiu, Y., Fu, B.J., Wang, J., Chen, L.D., 2001. Soil moisture variation in relation to topography and land use in a hillslope catchment of the Loess Plateau, China. J. Hydrol. 240, 243–263. https://doi.org/10.1016/S0022-1694(00)00362-0.

Rodriguez-Caballero, E., Canton, Y., Chamizo, S., Lazaro, R., Escudero, A., 2013. Soil loss and runoff in semiarid ecosystems: a complex interaction between biological soil crusts, micro-topography, and hydrological drivers. Ecosystems 16, 529–546. https://doi.org/10.1007/s10021-012-9626-z.

Sarstedt, M., Hair, J.F., Ringle, C.M., Kai, O.T., Gudergan, S.P., 2016. Estimation issues with PLS and CBSEM: where the bias lies! J. Bus. Res. 69, 3998–4010. https://doi.org/10.1016/j.jbusres.2016.06.007.

Saygin, S.D., Huang, C.H., Flanagan, D.C., Erpul, G., 2018. Process-based soil erodibility estimation for empirical water erosion models. J. Hydraul. Res. 56, 181–195. https://doi.org/10.1080/00221686.2017.1312577.

Sheridan, G.J., So, H.B., Loch, R.J., Walker, C.M., 2000. Estimation of erosion model erodibility parameters from media properties. Aust. J. Soil Res. 38, 265–284. https://doi.org/10.1071/SR99041.

Shit, P.K., Maiti, R., 2012. Effects of plant root density on the erodibility of lateritic topsoil by simulated flume experiment. Int. J. For. Soil Eros. 2, 137–142.

Six, J., Bossuyt, H., Degryze, S., Denef, K., 2004. A history of research on the link between (micro)aggregates, soil biota, and soil organic matter dynamics. Soil Tillage Res. 79, 7–31. https://doi.org/10.1016/j.still.2004.03.008.

Song, X., Tang, G., Li, F., Jiang, L., Zhou, Y., Qian, K., 2013. Extraction of loess shoulder-line based on the parallel GVF snake model in the loess hilly area of China. Comput. Geosci. 52, 11–20. https://doi.org/10.1016/j.cageo.2012.08.014.

Sun, L., Zhang, G.H., Luan, L.L., Liu, F., 2016. Temporal variation in soil resistance to flowing water erosion for soil incorporated with plant litters in the Loess Plateau of China. Catena 145, 239–245. https://doi.org/10.1016/j.catena.2016.06.016.

Vannoppen, W., Vanmaercke, M., De Baets, S., Poesen, J., 2015. A review of the mechanical effects of plant roots on concentrated flow erosion rates. Earth Sci. Rev. 150, 666–678. https://doi.org/10.1016/j.earscirev.2015.08.011.

Walia, M.K., Dick, W.A., 2018. Selected soil physical properties and aggregate-associated carbon and nitrogen as influenced by gypsum, crop residue, and glucose. Geoderma 320, 67–73. https://doi.org/10.1016/j.geoderma.2018.01.022.

Wang, B., Zhang, G.H., 2017. Quantifying the binding and bonding effects of plant roots on soil detachment by overland flow in 10 typical grasslands on the Loess Plateau. Soil Sci. Soc. Am. J. 81, 1567–1576. https://doi.org/10.2136/sssaj2017.07.0249.

Wang, B., Zhang, G.H., Shi, Y.Y., Zhang, X.C., Ren, Z.P., Zhu, L.J., 2013. Effect of natural restoration time of abandoned farmland on soil detachment by overland flow in the Loess Plateau of China. Earth Surf. Process. Landf. 38, 1725–1734. https://doi.org/10.1002/esp.3459.

Wang, B., Zhang, G.H., Shi, Y.Y., Zhang, X.C., 2014. Soil detachment by overland flow under different vegetation restoration models in the Loess Plateau of China. Catena 116, 51–59. https://doi.org/10.1016/j.catena.2013.12.010.

Wang, B., Zhang, G.H., Yang, Y.F., Li, P.P., Liu, J.X., 2018b. Response of soil detachment capacity to plant root and soil properties in typical grasslands on the Loess Plateau. Agric. Ecosyst. Environ. 266, 68–75. https://doi.org/10.1016/j.agee.2018.07.016.

Wang, H., Zhang, G.H., 2021. Temporal variation in soil erodibility indices for five typical land use types on the Loess Plateau of China. Geoderma 381, 114695. https://doi.org/10.1016/j.geoderma.2020.114695.

Wang, H., Zhang, G.H., Li, N.N., Zhang, B.J., Yang, H.Y., 2018a. Soil erodibility influenced by natural restoration time of abandoned farmland on the Loess Plateau of China. Geoderma 325, 18–27. https://doi.org/10.1016/j.geoderma.2018.03.037.

Wang, H., Zhang, G.H., Li, N.N., Zhang, B.J., Yang, H.Y., 2019a. Variation in soil erodibility under five typical land uses in a small watershed on the Loess Plateau, China. Catena 174, 24–35. https://doi.org/10.1016/j.catena.2018.11.003.

Wang, J., Feng, S., Ni, S., Wen, H., Cai, C., Guo, Z., 2019b. Soil detachment by overland flow on hillslopes with permanent gullies in the Granite area of southeast China. Catena 183, 104235. https://doi.org/10.1016/j.catena.2019.104235.

Wei, W., Chen, L.D., Fu, B.J., Huang, Z.L., Wu, D.P., Gui, L.D., 2007. The effect of land uses and rainfall regimes on runoff and soil erosion in the semi-arid loess hilly area, China. J. Hydrol. 335, 247–258. https://doi.org/10.1016/j.jhydrol.2006.11.016.

Williams, J.R., Arnold, J.G., 1997. A system of erosion—sediment yield models. Soil Technol. 11, 43–55. https://doi.org/10.1016/S0933-3630(96)00114-6.

Wu, G.L., Liu, Y., Fang, N.F., 2016. Soil physical properties response to grassland conversion from cropland on the semiarid area. Ecohydrology 9, 1471–1479. https://doi.org/10.1002/eco.1740.

Wu, X., Wei, Y., Wang, J., Cai, C., Deng, Y., Xia, J., 2018. RUSLE erodibility of heavy-textured soils as affected by soil type, erosional degradation, and rainfall intensity: a field simulation. Land Degrad. Dev. 29, 408–421. https://doi.org/10.1002/ldr.2864.

Xia, L., Song, X.Y., Fu, N., Li, H.Y., Li, Y.L., 2017. Impacts of land use change and climate variation on green water in the Loess Plateau Gully Region—a case study of Nanxiaohegou basin. J. Hydraul. Eng. 48, 678–688 (in Chinese). 10.13243/j.cnki.slxb.20160900.

Yu, D.S., Shi, X.Z., Weindorf, D.C., 2006. Relationships between permeability and erodibility of cultivated Acrisols and Cambisols in subtropical China. Pedosphere 16, 304–311. https://doi.org/10.1016/S1002-0160(06)60056-8.

Zhang, B.J., Zhang, G.H., Yang, H.Y., Wang, H., 2019. Soil resistance to flowing water erosion of seven typical plant communities on steep gully slopes on the Loess Plateau of China. Catena 173, 375–383. https://doi.org/10.1016/j.catena.2018.10.036.

Zhang, K., Lian, L., Zhang, Z., 2016. Reliability of soil erodibility estimation in areas outside the us: a comparison of erodibility for main agricultural soils in the US and China. Environ. Earth Sci. 75, 252. https://doi.org/10.1007/s12665-015-4980-8.
Zhang, K.L., Shu, A.P., Xu, X.L., Yang, Q.K., Yu, B.F., 2008. Soil erodibility and its estimation for agricultural soil in China. J. Arid Environ. 72, 1002–1011. https://doi.org/10.1016/j.jaridenv.2007.11.018.
Zhao, A.C., 1994. Analysis of control models of typical small watershed in gully area of Loess Plateau, the east part of Gansu Province. Research of Soil and Water Conservation, pp. 45–49 (In Chinese).
Zhu, B.B., Li, Z.B., Li, P., Liu, G., Xue, S., 2010. Soil erodibility, microbial biomass, and physical–chemical property changes during long-term natural vegetation restoration: a case study in the Loess Plateau, China. Ecol. Res. 25, 531–541. https://doi.org/10.1007/s11284-009-0683-5.
Zhu, G., Deng, L., Shangguan, Z., 2018. Effects of soil aggregate stability on soil N following land use changes under erodible environment. Agric. Ecosyst. Environ. 262, 18–28. https://doi.org/10.1016/j.agee.2018.04.012.
Zhu, H.C., Tang, G.A., Zhang, Y.S., Yi, H.W., Li, M., 2003. Thalweg in Loess Hill area based on DEM. Bull. Soil Water Conserv. 23, 43–45 61. (in Chinese). 10.13961/j.cnki.stbctb.2003.05.011.
Ziadat, F.M., Taimeh, A.Y., Hattar, B.I., 2010. Variation of soil physical properties and moisture content along toposequences in the arid to semiarid area. Arid Land Res. Manag. 24, 81–97. https://doi.org/10.1080/15324981003635396.